Journal Pre-proof


# Acute SARS-CoV-2 infection impairs dendritic cell and T cell responses

Runhong Zhou, Kelvin Kai-Wang To, Yik-Chun Wong, Li Liu, Biao Zhou, Xin Li, Haode Huang, Yufei Mo, Tsz-Yat Luk, Thomas Tsz-Kan Lau, Pauline Yeung, Wai-Ming Chan, Alan Ka-Lun Wu, Kwok-Cheung Lung, Owen Tak-Yin Tsang, Wai-Shing Leung, Ivan Fan-Ngai Hung, Kwok-Yung Yuen, Zhiwei Chen

PII: S1074-7613(20)30333-2

DOI: https://doi.org/10.1016/j.immuni.2020.07.026

Reference: IMMUNI 4434

To appear in: *Immunity*

Received Date: 19 May 2020

Revised Date: 24 June 2020

Accepted Date: 27 July 2020

Please cite this article as: Zhou, R., Kai-Wang To, K., Wong, Y.-C., Liu, L., Zhou, B., Li, X., Huang, H., Mo, Y., Luk, T.-Y., Tsz-Kan Lau, T., Yeung, P., Chan, W.-M., Ka-Lun Wu, A., Lung, K.-C., Tak-Yin Tsang, O., Leung, W.-S., Fan-Ngai Hung, I., Yuen, K.-Y., Chen, Z., Acute SARS-CoV-2 infection impairs dendritic cell and T cell responses, *Immunity* (2020), doi: https://doi.org/10.1016/j.immuni.2020.07.026.

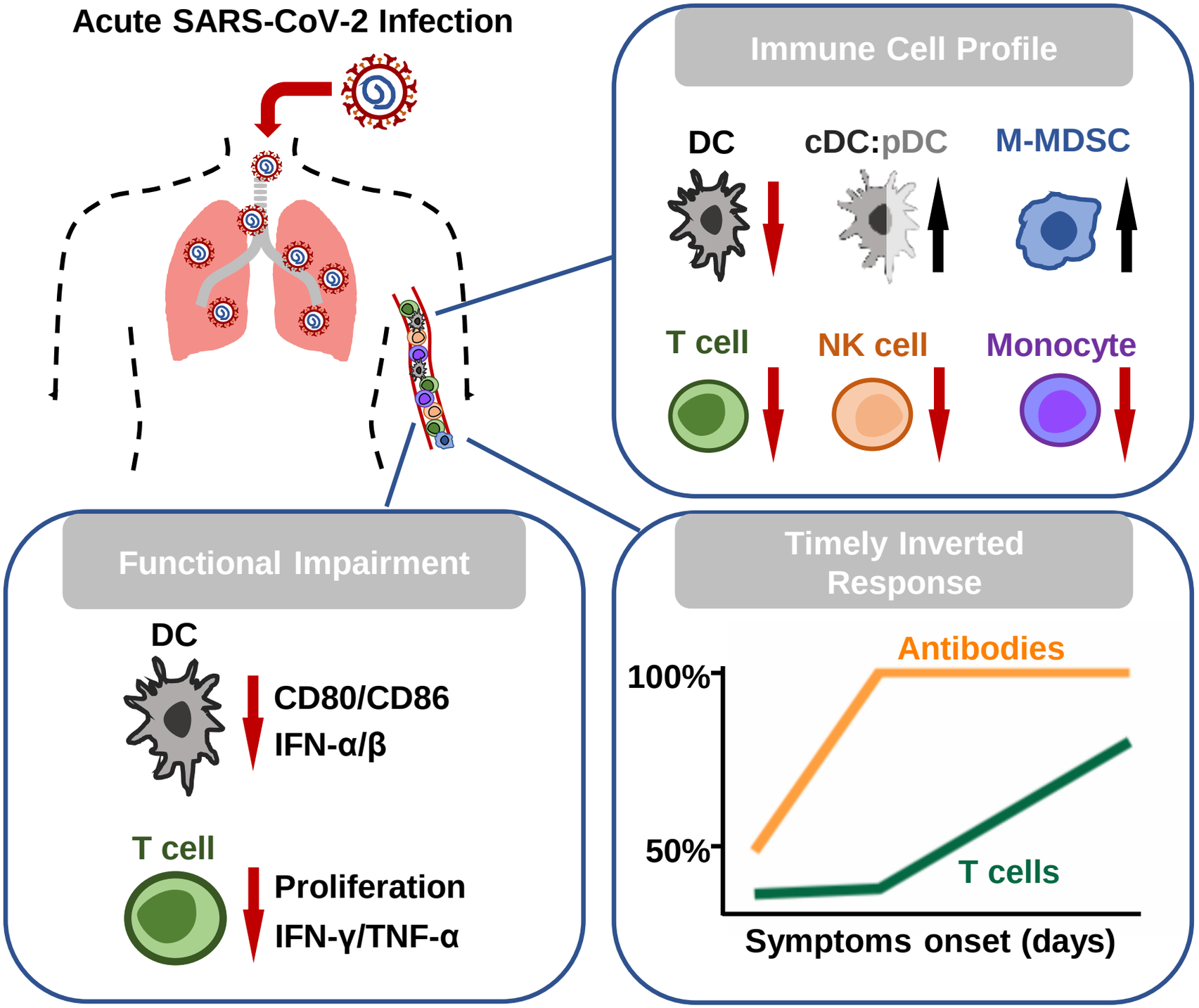
Acute SARS-CoV-2 Infection
Immune Cell Profile
DC
cDC:pDC
M-MDSC
T cell
NK cell
Monocyte
Functional Impairment
DC
CD80/CD86
IFN-α/β
T cell
Proliferation
IFN-γ/TNF-α
Timely Inverted Response
Antibodies
100%
50%
T cells
Symptoms onset (days)

# Acute SARS-CoV-2 infection impairs dendritic cell and T cell responses

Runhong Zhou[1,2,9], Kelvin Kai-Wang To[2,9], Yik-Chun Wong[1,2,9], Li Liu[1,2,9], Biao Zhou[1,2,9], Xin Li[1], Haode Huang[1], Yufei Mo[1,2], Tsz-Yat Luk[1], Thomas Tsz-Kan Lau[1], Pauline Yeung[3], Wai-Ming Chan[4], Alan Ka-Lun Wu[5], Kwok-Cheung Lung[6], Owen Tak-Yin Tsang[7], Wai-Shing Leung[7], Ivan Fan-Ngai Hung[8], Kwok-Yung Yuen[2]* and Zhiwei Chen[1,2,10]*

[1]AIDS Institute, Li Ka Shing Faculty of Medicine, The University of Hong Kong, Hong Kong Special Administrative Region (SAR), People's Republic of China;

[2]Department of Microbiology, State Key Laboratory of Emerging Infectious Diseases, Li Ka Shing Faculty of Medicine, The University of Hong Kong, Hong Kong SAR, People's Republic of China;

[3]Department of Intensive Care, Queen Mary Hospital, The University of Hong Kong, Hong Kong SAR, People's Republic of China;

[4]Department of Adult Intensive Care, Queen Mary Hospital, Hong Kong SAR, People's Republic of China;

[5]Department of Microbiology, Pamela Youde Nethersole Eastern Hospital, Hong Kong SAR, People's Republic of China;

[6]Department of Medicine, Pamela Youde Nethersole Eastern Hospital, Hong Kong SAR, People's Republic of China;

[7]Department of Medicine, Princess Margaret Hospital, Hong Kong SAR, People's Republic of China;

[8]Department of Medicine, Li Ka Shing Faculty of Medicine, The University of Hong Kong, Hong Kong SAR, People's Republic of China

[9]These authors made equal contributions

[10]Lead Contact

*Correspondence to: Zhiwei Chen (Lead contact), E-mail: zchenai@hku.hk and Kwok-Yung Yuen, E-mail: kyyuen@hku.hk. Department of Microbiology, Li Ka Shing Faculty of Medicine, The University of Hong Kong, L5-45, 21 Sassoon Road, Pokfulam, Hong Kong SAR, People's Republic of China. Phone: 852-3917-9831; Fax: 852-3917-7805.

The authors declared no conflict of interests.

**Summary**

The SARS-CoV-2 pandemic has resulted in millions of infections yet the role of host immune responses in early COVID-19 pathogenesis remains unclear. By investigating 17 acute and 24 convalescent patients, we found that acute SARS-CoV-2 infection resulted in broad immune cell reduction including T, NK, monocyte and dendritic cell (DC). DCs were significantly reduced with functional impairment, and cDC:pDC ratios were increased among acute severe patients. Besides lymphocytopenia, although neutralizing antibodies were rapidly and abundantly generated in patients, there were delayed receptor binding domain (RBD)- and nucleocapsid protein (NP)-specific T cell responses during the first 3 weeks post symptoms onset. Moreover, acute RBD- and NP-specific T cell responses included relatively more CD4 T cells than CD8 T cells. Our findings provided evidence that impaired DCs, together with timely inverted strong antibody but weak CD8 T cell responses, may contribute to acute COVID-19 pathogenesis and have implications for vaccine development.

**Keywords:** SARS-CoV-2; COVID-19; acute infection; convalescent; dendritic cell; receptor-binding domain; nucleocapsid protein; neutralizing antibody; T cell immune response

## Introduction

In December 2019, the Coronavirus disease 2019 (COVID-19) outbreak was discovered among a group of pneumonia patients mainly associated with a seafood market in Wuhan city, China (Zhu et al., 2020). The pandemic was suspected to be zoonotic and to have originated from a novel beta-coronavirus (CoV) that is now officially named as SARS-CoV-2 (Qian et al., 2020; Zhu et al., 2020). SARS-CoV-2 is similar to bat SARS-related coronaviruses with 96% genomic identity, but it is relatively distinct from SARS-CoV that only has 79.5% similarity (Liu et al., 2020; Wu et al., 2020). The rapid dissemination of SARS-CoV-2 was related to highly efficient person-to-person transmissions in both hospital and community settings (Liu et al., 2020; Wang et al., 2020a). SARS-CoV-2 has been spread globally by travellers, often through contact with asymptomatic carriers (Holshue et al., 2020; Rothe et al., 2020). Since then, COVID-19 has become a severe worldwide pandemic with over fifteen million confirmed cases and around 617,000 deaths within six months. It remains unclear why host immune responses are insufficient in controlling early pathogenesis and the transmission of SARS-CoV-2. Therefore, it is crucial to dissect the immune mechanisms to promote the control of the pandemic and the development of an effective vaccine against COVID-19.

Several elegant studies demonstrated that SARS-CoV-2 and SARS-CoV use the same cellular entry receptor angiotensin-converting enzyme 2 (ACE2) to initiate infection, despite that only 40% amino acids are identical in the receptor binding domain (RBD) external subdomain (Chan et al., 2020a; Wan et al., 2020). Since other coronaviruses also use ACE2 as the cellular receptor but have not caused any major outbreaks, it is suspected that other host factors besides ACE2 may contribute to the highly efficient zoonotic and person-to-person transmission of SARS-CoV-2 (Chen et al., 2020b; Huang et al., 2020). Currently, the mechanism underlying early immunopathogenesis of COVID-19 remains unclear and is yet to be fully determined.

It is known that host immune responses play a critical role in defending against viral infection and disease progression (Ho et al., 2005; Zhao et al., 2010). A reduced innate and adaptive immune response can cause harm especially during the acute phase of infection (Ho et al., 2005). We previously demonstrated that spike (S)-specific antibodies, which even contain neutralizing antibodies (NAb), may cause acute lung injury upon live SARS-CoV infection in

both SARS patients and non-human primates (NHP) (Liu et al., 2019; Zhang et al., 2006). Recently, COVID-19 patients with higher amounts of anti-nucleocapsid (NP) IgM and IgG following symptoms onset have been associated with poorer disease outcomes (Tan et al., 2020). In another study, higher amounts of anti-S and anti-NP IgG and IgM were correlated with worse clinical readouts and older age (Jiang et al., 2020). Besides humoral responses, T lymphocytopenia is inversely correlated with an increase of peripheral pro-inflammatory cytokines among COVID-19 patients (Chiappelli et al., 2020; Xu et al., 2020; Zheng et al., 2020). The low $CD8^+$ T cell count has been suggested to be a predictor for high mortality and illness severity of COVID-19 pneumonia (Du et al., 2020; Xu et al., 2020). On the other hand, low $CD4^+$ T cell count was independently associated with intensive care unit (ICU) admission (Chen et al., 2020a). These findings support a hypothesis that unbalanced adaptive immune responses may potentially have detrimental effects on acute COVID-19 patients. To address this hypothesis, while recent studies have focused on the importance of T cell immunity in convalescent patients (Grifoni, 2020; Ni et al., 2020), we sought to investigate the functionality of different innate and adaptive immune cells and the adaptive immune responses in both acute and convalescent patients. We found that SARS-CoV-2 rapidly impaired dendritic cell and T cell responses during the acute phase of infection, which may have significant implications for COVID-19 pathogenesis.

## Results

### Clinical characteristics of COVID-19 patients

Between 10th February and 22nd April 2020, a total of 41 COVID-19 subjects, including 8 severe and 33 mild patients (24 female and 17 male), with sufficient blood samples were screened and recruited into our study (Table 1). Initially, 6 severe and 11 mild cases were recruited in the acute patients (AP) group (recruited during hospitalization), while 2 severe and 22 mild patients were included in the convalescent patients (CP) group (recruited at follow-up outpatient clinic). After hospital discharge, 5 AP subjects were subsequently recruited for experiments with CP. When we analysed patients' profiles listed in Table 1, no significant differences were observed between AP and CP groups at the time of hospital admission (Table S1). We then divided our study subjects into mild and severe patient groups (Table 1). Oxygen supplementation were all required in the 8 considered as severe COVID-19 patients, whereas the rest of the 33 patients only presented mild symptoms. The median age of severe and mild patients was 59 years old (interquartile range 54-69) and 57

years old (interquartile range 33-63), respectively. Among the 41 patients, chronic comorbidities were more common among the severe group (6/8, 75%) than the mild group (9/33, 27%) (P=0.035). The most common underlying diseases were hypertension in 8/41 (20%) and diabetes mellitus in 5/41 (12%) patients. Hypertension was significantly more frequent amongst severe than mild patients (4/8, 50% vs 4/33, 12.1%; p=0.033) and so was diabetes mellitus (3/8, 37.5% vs 2/33, 6.1%; p=0.043). Regarding symptoms presentation, fever (23/41, 56%) was the most common, followed by cough (16/41, 39%), sore throat (6/41, 15%) and dyspnea (5/41, 12%) (Table 1). Dyspnea was significantly more frequent amongst severe than mild patients (3/8, 37.5% vs 2/33, 6.1%; p=0.043). For blood tests performed at admission, lymphocyte counts in severe patients were significantly lower than in mild patients ($0.9\times10^9$ cells/L [range 0.8-0.9] vs 1.2 [1.0-1.6]; p=0.011). Similarly, severe patients had a significantly lower platelet count than mild patients ($150\times10^9$ cells/L [range 141-191] vs 236 [184-309]; p=0.002). These results demonstrated that acute SARS-CoV-2 infection could lead to a more profound immune suppression in severe patients.

**Acute SARS-CoV-2 infection results in broad reduction of different immune cell populations**

Using two panels of antibodies for 12-color flow cytometry analysis (Table S2), we evaluated immune cell profiles of AP and CP as compared with those of healthy donors (HD). Freshly isolated human PBMCs were subjected to the flow cytometry analysis using gating strategies presented in Figure S1A and S2, except for 5 AP frozen samples. We observed significantly reduced frequencies of broad immune cell types, including T cell, NK cell, dendritic cell (DC) and classical monocyte in AP as compared with HD (Figure 1A and 1B). These 5 AP frozen samples displayed slightly high % T cells, which did not affect overall statistical analysis. In contrast, the frequency of monocytic myeloid-derived suppressive cells (M-MDSCs) was significantly higher in AP than that in HD. Since the majority of AP samples (14/17) were tested within 3 weeks after symptoms onset (6 in 1-7 days, 5 in 8-14, 3 in 15-21, 3 in >21), our observation on immune cell profiling indicated that acute SARS-CoV-2 infection resulted in broad immune cell reduction during the early phase of infection. Of note, while many CP had increased frequencies of lymphocytes including T and NK cells (Figure 1A), their frequencies of DC and monocyte remained significantly lower than those of HD (Figure 1B). These observations suggested that there was likely a broad suppression of monocyte and DC populations with shorter-term effect on NK and T cells in COVID-19 patients.

**AP-derived DCs have reduced frequency and functionality for undergoing maturation**

DCs play a central role in both innate and adaptive immune responses. Moreover, plasmacytoid DCs (pDCs) comprise a subset of DCs characterized by their ability to produce large amount of antiviral type I interferon (IFN-I) (Fitzgerald-Bocarsly et al., 2008). We therefore further measured the proportion and functionality of conventional dendritic cell (cDC) and pDC subsets among total DCs derived from our AP and CP patients. The frequencies of $CD11c^+$ cDCs in total DCs showed increases in CP group (Figure 2A, top panel and Figure S2A). Moreover, there were significant increases of the cDC:pDC ratios in the AP group as compared with the HD and CP groups. We then compared DC surface markers (HLA-DR, CD86 and CCR2) and functionality among our study subjects. The expression amount of the co-stimulatory molecule CD86 was significantly lower in both AP and CP than that in HD (Figure 2A, bottom panel), whereas there were no differences for HLA-DR or CCR2. These results indicated that patient-derived DCs might reduce their functionality of maturation. To test this hypothesis, we then measured the effect of a cocktail of maturation cytokines (IL-1β, IL-6, TNF-α and PGE2) on patient-derived cDCs isolated from 3 AP and 4 CP based on the availability of samples. The results of real-time RT-PCR showed that there are no significant differences in receptor expression of IL-6 (IL-6R), TNF-α (TNFR1/2) and PGE2 (EP2) between HD and COVID-19 patients (data not shown). The maturation cytokine cocktail was added to stimulate freshly isolated DCs for 24 hours, after which the expression levels of the maturation markers on cDCs ($CD11c^+$) was determined by flow cytometry using the DC maturation panel of antibodies (Figure S2B and Table S2). The maturation stimuli significantly upregulated the co-stimulatory molecules CD80 and CD86 in all HD (Figure 2B, top panel) but not CD83, CCR7, HLA-ABC and HLA-DR molecules (data not shown). The increase in DC maturation, however, was not significant in 3/3 AP and 1/4 CP. In these DC cultures, IFN-α were not induced in 3/3 AP and 3/4 CP, whereas IFN-β were not significantly increased in 3/3 AP, rather only slightly elevated in 3/4 CP (Figure 2B, bottom panel), indicating a reduced capacity of making antiviral interferon, especially among APs. In addition, significantly less CD80, CD86, CCR7 and HLA-DR expression were induced in all three subsets of peripheral dendritic cells (pDCs, cDC1 and cDC2) in 3/3 AP after stimulation with TLR3, 4, 7 or 8 ligands as compared with HD (Figure S3). We next conducted the mixed lymphocyte reaction assay (MLR) to further determine the functionality of patient-derived DCs to induce proliferation of allogeneic CD4 and CD8 T cells at both immature and maturation stages (Jongbloed et al., 2010). While HD- and CP-derived DCs

were able to stimulate CD4 and CD8 T cell proliferation, none of the AP-derived DCs displayed similar activity (Figure 2C). These results demonstrated that DCs derived from AP are functionally impaired for maturation and T cell activation, thereby likely reduce induction of adaptive T cell responses against SARS-CoV-2.

**AP-derived peripheral CD4 and CD8 T cells display reduced functionality**

Antigen-specific T cells are responsible for SARS-CoV clearance and host survival (Zhao et al., 2010). Since acute SARS-CoV-2 infection resulted in T lymphocytopenia, we sought to determine the phenotype and functionality of patient-derived CD4 and CD8 T cells. Phenotypic analysis by measuring Ki67 expression showed that T lymphocytopenia was likely associated with the significant reduction of CD4 T cell proliferation (Figure 3A and Figure S1B). Evaluating CD38 and HLA-DR expression during acute infection also associated T lymphocytopenia with elevated activation of CD8 T cells (Figure 3A and Figure S1A). However, the frequency of total % T cells was positively correlated with only $Ki67^+$ CD4 T cells among AP but not with activated $CD38^+HLA\text{-}DR^+$ CD8 (Figure S4). Interestingly, most AP and CP patients' CD4 T but not CD8 T cells expressed higher amount of PD-1 than that of HD, indicating a state of CD4 activation or possible exhaustion. We then performed *ex vivo* experiments to measure T cell proliferation in 6 AP and 6 CP through T cell receptor (TCR) activation by anti-CD3 and anti-CD28 antibodies as compared with HD. AP-derived CD4 and CD8 T cells showed significantly reduced frequencies of CSFE cells (Figure 3B, top panel) and lower capacity for producing IFN-γ and IL-2 (Figure 3B, bottom panel). Furthermore, performing polyclonal stimulation with PMA/Ionomycin revealed that both central memory (CM) and effector memory (EM) CD4 T cells have significantly reduced polyfunctionality for releasing both IFN-γ and TNF-α in 6 AP as compared with that of CP and HD (Figure 3C, middle panel). Similarly, EM and $CD45RA^+$ effector (EMRA) CD8 T cells also showed reduced polyfunctionality for releasing both IFN-γ and TNF-α in 6 AP as compared with that of CP and HD (Figure 3C, bottom panel). In addition, in the absence of any stimulation, EM and EMRA CD8 T cells of 6/6 AP also displayed significantly reduced cytotoxic potential for expressing granzyme B and perforin (Figure 3D). These findings demonstrated that acute SARS-CoV-2 infection has led to functional impairment in both CD4 and CD8 T cell subsets in AP patients.

**Impact of disease severity on AP-derived immune cells**

To further evaluate the impact of disease severity on patients' immune cell profiles at the acute stage of SARS-CoV-2 infection, we divided the AP group into mild and severe patients for comparison. Interestingly, the frequency of M-MDSCs was significantly higher in severe patients than that of mild ones (Figure 4A). There were no significant differences for other immune cell types including T, B, NK, DC and monocytes between mild and severe patients. Moreover, there were no significant differences for expression of Ki67, PD-1 and $CD38^{+}$HLA-DR in both CD4 and CD8 T cells (Figure S5). When DC subsets were further analyzed, however, there was a significant increase of the cDC:pDC ratio in severe patients than that in mild ones (Figure 4B, top panel) although significant differences were not found for the frequencies of cDC and pDC. In addition, there were no significant differences in HLA-DR, CD86 and CCR2 expression on cDC between mild and severe patients (Figure 4B, bottom panel). These findings suggested that acute SARS-CoV-2 infection results in more significant changes in cDC:pDC ratios and the increase of M-MDSCs among severe patients. High cDC:pDC ratios of about 50-fold may serve as a potential biomarker of severe sickness.

**Timely inverted RBD-specific antibody and T cell responses in AP**

Upon viral entry, earlier development of antigen-specific T cells and subsequent production of neutralizing antibodies (NAb) are classical adaptive immune responses for effective control of infection and elimination of pathogens (Chaplin, 2010). To further study specific immunity in AP, we developed ELISA and pseudovirus-based neutralization assays to measure antibody responses, as well as ELISPOT to measure cell-mediated immune responses. In the first week after symptoms onset, specific RBD IgG responses were found in 4/7 mild AP (P2, P3, P4 and P7) by ELISA. Three of them developed high NAb titers but low NP-specific T cell responses, whereas only 2 of them had weak RBD-specific T cells (Figure 5A). Only P4 had NP-specific T cells with > 500 spots/million PBMC. In the second week after symptoms onset, 8/8 AP, including 4 mild and 4 severe cases, developed both RBD IgG and Nab responses. Importantly, however, 4/4 severe patients (P8, P10, P11 and P13) did not develop measurable T cell responses against NP or RBD. In contrast, two mild followed-up cases P3 and P4 displayed increased NP- but not RBD-specific T cells while P3 developed NAb response at this stage. Another mild case P12 had RBD IgG and NAb responses but weak NP- and RBD-specific T cell responses (< 100 spots/million PBMC). In the third week and beyond, 4 AP were newly recruited including 2 severe cases (P16 and P17) and 2 mild cases (P14 and P15) whereas the rest were followed-up patients. During this stage, all AP had RBD IgG and NAb responses. Most AP also developed

increased NP-specific T cell responses except for the mild P14 and the severe P16 who did not have measurable T cell responses against NP and RBD. Notably, 3/5 followed-up patients including P7, P8 and P10 developed RBD-specific but weak T cell responses. Our results, therefore, demonstrated that the overall frequencies of RBD IgG and NAb responses in AP reached 100% (8/8) by the second week after symptom onset, whereas only 50% (4/8) and 25% (2/8) were found for NP- and RBD-specific T cell responses, respectively (Figure 5B, left). When the AP group was divided to compare mild versus severe cases, 4/4 and 2/4 mild AP had NP- and RBD-specific T cell responses (Figure 5B, middle). In contrast, none of the 4/4 severe AP developed NP- and RBD-specific T cell responses at this stage (Figure 5B, right), indicating that delayed cell-mediated immune responses may contribute to acute COVID-19 pathogenesis.

To understand the possible immune responses that are associated with viral clearance, we labelled each severe AP with a black symbol for kinetic analysis (Figure 5C). In week two after symptoms onset, although 4/4 mild and 4/4 severe AP developed comparable amounts of RBD IgG and Nab responses, 1/4 mild and 3/4 severe cases still had viral loads ($>10^5$ copies/ml). At the same time, 4/4 mild and 0/4 severe AP had NP ELISPOT responses. Moreover, significantly higher numbers of NP ELISPOT responses were found in AP without detectable viral loads than in those with measurable viral loads (Figure 5D). Improved immune responses over time were observed when we plotted four AP patients (2 mild and 2 severe) who have multiple samples collected consecutively (Figure S6). These results implicated that NP-specific T cells are likely needed for reducing disease severity and viral control during acute infection.

**Higher frequencies of effector memory CD4 than CD8 T cell responses against NP and RBD**

We lastly evaluated antibody and T cell responses in 23 CP at a median of 30 days after symptoms onset (range, 21-54 days). All CP (100%, 23/23) developed both anti-RBD IgG and neutralizing antibodies, while 61% (14/23) and 83% (19/23) of them developed RBD- and NP-specific T cell responses, respectively (Figure 6A). Moreover, when RBD peptide pool and RBD protein were compared using the same ELISPOT, consistent responses were observed with a significantly positive correlation (Figure S7). Based on availability of isolated cells, we also determined specific T cell responses in CD4 and CD8 subsets by ICS in 3 AP and 13 CP. Significantly higher frequencies of T cell responses were found in CD4

than in CD8 T cells against both RBD and NP (Figure 6B). Moreover, consistent with the ELISPOT results, the frequencies of NP-specific T cell responses were higher than RBD-specific T cell responses, which is similar to a recent study of CP subjects (Ni et al., 2020). Interestingly, the majority of NP- and RBD-specific CD4 T cells tended to have an effector memory (EM) phenotype (Figure 6C). NP- and RBD-specific but weaker CD8 T cells also exhibited the effector memory (EM) phenotype (Figure S8A). Interestingly, when all 51 samples from 17 AP and 23 CP were analysed together, there was a strong positive correlation between RBD IgG and NAb responses (Figure S8B) as well as between RBD-specific T cell response and NAb titer (Figure S8C). The development of NAb, therefore, may still be correlated with the induction of RBD-specific T cells responses. In contrast, the correlation between NP RBD-specific T cell response and NAb titer did not reach statistical significance (Figure S8D). Our results indicated that timely inverted strong antibody but weak CD8 T cell responses might be immune features of acute SARS-CoV-2 infection.

**Discussion**

Rapid loss of DC function may lead to delayed T cell immune responses in COVID-19 patients. DC plays an important role in bridging innate and adaptive immunity. Neither DCs nor macrophages are permissive for SARS-CoV replication (Tseng et al., 2005). The infection was abortive because there was no increase in viral RNA and viral titer. Infected DCs neither produced anti-viral cytokines nor matured to perform direct antigen presentation to activate T cells (Law et al., 2005). In NHP, we showed that mucosal monocytes/macrophages sequestered SARS-CoV virions in intracellular vesicles together with infected Langerhans cells (Liu et al., 2016). They then migrated into the tonsils and/or draining lymph nodes, all within 2 days of infection. In lymphoid tissues, viral RNA and proteins were detected in infected monocytes upon differentiation into DCs within 3 days. Therefore, spatiotemporal interactions of SARS-CoV, monocytes/macrophages, and the DC network in mucosal tissues provide a mechanism for the virus to escape host mucosal innate immunity and disseminate systemically (Liu et al., 2016). Among SARS patients, the frequency of peripheral DC subsets significantly dropped after symptoms onset, mainly attributed to a large dose of steroid administration (Zhang et al., 2004). In this study, although few of our AP COVID-19 patients received even low dose steroid treatment, the frequency and functionality of peripheral DC subsets still significantly and rapidly reduced upon symptoms onset. On the one hand, pDC is the major potent type-I interferon producer

upon viral infection. Therefore, the significant loss of pDC, together with NK cells reduction among severe cases may lead to immediate abolishment of innate immunity against SARS-CoV-2 infection. To this end, SARS-CoV-2 significantly suppressed the host innate immune response in *ex vivo* human lung tissue explant compared with 2003 SARS-CoV (Chu et al., 2020). These implicated the significant efficacy of our early interferon beta-1b cocktail treatment (Hung et al., 2020). Our results also suggested that a high ratio of cDC:pDC at about 50-fold may serve as a potential biomarker for severe sickness. For one exception, the severe AP (P8) who had a low ratio of cDC:pDC during acute infection was actually able to develop early NP-specific T cell responses. On the other hand, the rapid loss of dendritic cell number and function may contribute to the delayed T cell responses and the features of low level type I/III interferons during COVID-19 infection (Blanco-Melo et al., 2020).

Acute SARS-CoV-2 infection results in a loss of a predominant RBD-specific T cell response. Lymphocytopenia is a common clinical presentation of both SARS and COVID-19, and this suggests that the two viruses may share a common mechanism in immune evasion. Grifoni et al reported that the frequencies of T lymphocytes were not significantly low because their subjects were convalescing COVID-19 patients (Grifoni, 2020), who are similar to our CP cases. Liao et al showed recently that there were increased T cells in bronchoalveolar lavage fluids in mild patients but not in severe patients, suggesting a difference in T cell migration into the lungs (Liao et al., 2020). In our study, we found that reduced frequencies of peripheral T cells in AP subjects were likely associated with decreased CD4 T cell proliferation and CD8 T cell hyperactivation in addition to T cell migration into the lungs during acute infection. Most recovered SARS patients developed T cell immune responses that mainly target the spike glycoprotein when compared with non-structural proteins (Channappanavar et al., 2014; Li et al., 2008a; Lv et al., 2009; Wang et al., 2004; Xu and Gao, 2004). In particular, T cell responses against the RBD region had a high frequency of responders. T cell response against the single RBD epitope 435-NYNYKYRYLRHGKLRPF-451 was found among 22% convalescent subjects, only lower than 24% of an epitope in Orf3 (Li et al., 2008a). Memory CD8 T cells specific for a single immunodominant RBD epitope in this domain (S436) substantially protected 8- to 10-month-old mice from lethal SARS-CoV infection (Channappanavar et al., 2014). Importantly, this RBD epitope also contains the most important determinant for inducing NAbs. We previously demonstrated that a single R441A mutation eliminates vaccine-induced NAbs against SARS-CoV (Yi et al., 2005). Interestingly, despite that there is a high sequence variation in RBD between SARS-

CoV and SARS-CoV-2, the R441 residue remains conserved in both and allows the induction of RBD-specific NAbs. However, it is surprising that our AP subjects did not develop strong RBD-specific T cell response as evaluated by both ELISPOT and ICS assays. This aberrant observation contradicts with the high amounts of early RBD-specific IgG and NAb responses. This might be partly due to diminished DC function as mentioned above, or due to 7 amino acid differences (underlined) in the predicted immunodominant T cell epitope 435-NYNYLYRLFRKSNLKPF-451 in SARS-CoV-2. We also observed that 39% CP subjects did not develop measurable RBD-specific T cell responses. It is possible that lacking RBD-specific T cell responses might be one of the potential mechanisms allowing SARS-CoV-2 to evade immune control and results in prolonged viral shedding as compared with SARS-CoV.

Lack of timely developed CD8 T cell responses may contribute to disease severity during acute SARS-CoV-2 infection. The SARS-CoV infection induces strong and long-lasting cytotoxic T lymphocytes (CTL)-mediated immunity in surviving SARS patients (Chen et al., 2005). CD4-biased T cell responses induced by SARS-CoV, especially the proinflammatory cytokine storm, may cause pathological damage to the host (Xu and Gao, 2004). Moreover, increased Th2 cytokines were observed in patients with the fatal form of infection (Li et al., 2008a). We recently demonstrated that COVID-19 displays rapid kinetics of viral load peak and unexpected prolonged time of viral shedding in patients' salivary samples, which are different from what was seen in SARS patients (To et al., 2020). In this study, we found that besides the overall loss of T cell functionality during acute SARS-CoV-2 infection, both RBD- and NP-specific T cells were likely dominated by CD4 T cells. Since we were not able to obtain T cells from more severely ill patients in ICU for comparison, we could not establish the role of antigen-specific CD4 T cells in promoting COVID-19 disease severity. However, we found that 3/6 severe AP cases (P11, P13 and P16) had neither measurable CD4 nor CD8 T cell responses in contrast to their high amounts of potent NAb. In particular, although there is not a statistically significant difference in overall T cell responses between mild versus severe acute cases, the delayed RBD- and NP-specific T cell responses within first two weeks after symptoms onset might impact disease severity. It should be noted that initial T cell immune responses are highly variable among AP but they tend to improve over time. Overall, the unusual timely reverted NAb and T cell responses in acute patients might contribute to COVID-19 pathogenesis. In support of this notion, we and others have previously reported that deceased SARS patients had faster development of NAb than convalescent patients did (Ho et al., 2005; Zhang et al., 2006). Moreover, COVID-19

patients with higher amounts of anti-S, anti-N IgG and IgM correlate with worse clinical outcomes than patients with older age (Jiang et al., 2020). A recent preprint study indicated that SARS-CoV-2 NAb responses are more robust in patients with severe disease (Wang et al., 2020b), which agrees with our recent finding that severe AP subjects in ICU displayed significantly higher amounts of RBD IgG and NAb (Liu et al., 2020). In this study, although our overall AP and CP data indicated that the development of NAb may be correlated with the induction of RBD-specific T cells responses, which likely supports the notion that the production of NAbs by plasma B cells requires the priming of viral protein specific CD4 T cells (Grifoni, 2020; Mitchison, 2004), the underlying mechanism of faster NAb and delayed RBD-specific CD4 T cells response during acute infection remains to be investigated. In a recent study, Ni et al showed that 13/14 CP had NAb responses, where the numbers of RBD-specific T cells are much lower than those of NP-specific T cells by ELISPOT, and 3/8 and 1/8 CP did not have positive NP- and RBD-specific T cell responses, respectively (Ni et al., 2020). In a separate study, while 100% (20/20) CP developed RBD-specific antibody responses, peripheral SARS-CoV-2-specific $CD8^+$ and $CD4^+$ T cells were identified in ~70% and 100% of COVID-19 CP, respectively, using the T cell receptor-dependent activation induced marker (AIM) assay (Grifoni, 2020). Since this assay did not measure the antigen-specific intracellular cytokine production, whether or not the responses were overestimated remains to be further determined. Here, we demonstrated consistently that while 100% (23/23) CP had RBD IgG and NAb responses, 61% (14/23) and 83% (19/23) of them developed RBD- and NP-specific T cell responses, respectively. Moreover, 13% (3/23) CP had no measurable RBD- and NP-specific T cell responses against both NP and RBD. Collectively, the lack of T cell responses in some CP might indicate their possibility for prolonged viral transmission and their vulnerability to secondary infection.

There are some limitations in our experiments. Due to the limited number of severe COVID-19 patients in Hong Kong, the sample size of AP should be increased in future studies. Another possible drawback of our study is we used 15-mer overlapped by 11 for measuring RBD-specific CD4 T cell responses. CD4 T cell responses to larger peptides or conformational proteins therefore remain unclear. In addition, due to lymphocytopenia and other limitations of acquiring blood samples from ICU patients, the impact of NP- and RBD-specific T cell responses in COVID-19 disease severity should be further investigated by increasing sample size. Since antiviral treatment has been given to patients rapidly after hospital admission (Hung et al., 2020), future studies should evaluate the impact of such

therapy on host immune responses. Lastly, we only measured T cell responses to RBD and NP proteins, but T cell epitopes in the whole viral genome should be evaluated in future studies.

In summary, to the best of our knowledge, this study is the first to report DC functionality and imbalanced antibody and T cell responses during the acute phase of SARS-CoV-2 infection. We provide experimental evidence that acute SARS-CoV-2 infection leads to rapid deficiency of host DC and T cell functionality. This deficiency may have implications in viral pathogenesis, clinical severity, prolonged viral transmission and vulnerability for future re-infection. Our findings may importantly contribute to the current knowledge on acute COVID-19 pathogenesis and to the design of an effective vaccine for inducing balanced protective immunity.

**Acknowledgements**

This work was partly supported by Theme-Based Research Scheme (T11-706/18-N to ZC) of the Hong Kong Research Grants Council, University Development Fund and Li Ka Shing Faculty of Medicine Matching Fund from HKU to AIDS Institute. We thank Dr. Xu Aiming for providing purified NP protein. We also thank Serena J. Chen and Lok Yan Yim for editorial work. Funding supports to KY include the donations of the Shaw Foundation Hong Kong, Richard Yu and Carol Yu, May Tam Mak Mei Yin, Michael Seak-Kan Tong, Respiratory Viral Research Foundation Limited, Hui Ming, Hui Hoy and Chow Sin Lan Charity Fund Limited, Chan Yin Chuen Memorial Charitable Foundation, Marina Man-Wai Lee, the Hong Kong Hainan Commercial Association South China Microbiology Research Fund, the Jessie & George Ho Charitable Foundation, Perfect Shape Medical Limited, and Kai Chong Tong; and funding from the Health and Medical Research Fund (grant no. COVID190121 and CPVOD1901123), the Food and Health Bureau, The Government of the Hong Kong Special Administrative Region; the National Program on Key Research Project of China (grant no. 2020YFA0707500 and 2020YFA0707504); the Consultancy Service for Enhancing Laboratory Surveillance of Emerging Infectious Diseases and Research Capability on Antimicrobial Resistance for Department of Health of the Hong Kong Special Administrative Region Government; the Theme-Based Research Scheme (T11/707/15) of the Research Grants Council, Hong Kong Special Administrative Region; Sanming Project of Medicine in Shenzhen, China (No. SZSM201911014); and the High Level-Hospital Program,

Health Commission of Guangdong Province, China. The funding sources had no role in study design, data collection, analysis, interpretation, or writing of the report. The corresponding author had full access to all the data in the study and had final responsibility for the decision to submit for publication.

**Author Contributions**

ZC and K-YY supervised two collaborative teams in the study, respectively. RZ and ZC designed experiments, analysed data and wrote the manuscript. RZ, HH and YM did ELISPOT and ICS. Y-CW, RZ, XL, Y-LT and TT-KL prepared samples. LL and ZC conducted the pseudoviral neutralization assay. BZ did RBD ELISA. KK-WT, PY, W-MC, AK-LW, K-CL, OT-YT, W-SL and IF-NH collected clinical samples and data.

**DECLARATION OF INTERESTS**

The authors declare no competing interests.

**Figure legends**

**Figure 1. Acute SARS-CoV-2 infection results in broad immune cell suppression.** Fresh PBMCs were isolated from acute patients (AP), convalescent patients (CP) and healthy donors (HD). (**A**) For analysis of lymphocyte subsets including T, B and NK cells, samples of 17 AP and 25 CP were collected at a median of 13 (range, 1-42 days) and 30 days (range, 21-54 days) after symptoms onset, respectively. (**B**) For analysis of myeloid cells including DCs, $CD14^{++}CD16^{-}$ monocytes and MDSCs, samples of 17 AP and 29 CP were collected at a median of 13 (range, 1-42 days) and 30 days (range, 21-54 days) after symptoms onset, respectively. Twenty HD were included as controls. Cells were stained with different immune cell populations markers and subjected to flow cytometry analysis. Cumulative data showing the cell frequencies. Each symbol represents an individual donor with a line indicating the mean of each group. Severe patients in both AP and CP were presented as black symbols. Statistics were generated using one-way ANOVA followed by Tukey's multiple comparisons test and Mann–Whitney test. *$p<0.05$; **$p<0.01$, ***$p<0.001$.
See also Figure S1A, S2A and Table S1, S2.

**Figure 2. Dendritic cells derived from acute patients have reduced maturation potential.** (**A**) Flow cytometry analysis was used to define frequencies of $CD11c^+$ cDC and $CD123^+$ pDC in total blood DC, and the ratio of cDC:pDC. Samples of 17 AP and 29 CP were collected at a median of 13 (range, 1-42 days) and 30 days (range, 21-54 days) after symptoms onset, respectively. 20 HD were included as controls. The expression of HLA-DR, CD86 and CCR2 on cDCs were analysed using the mean fluorescence intensity (MFI). Samples of 17 AP and 24 CP were collected at a median of 13 (range, 1-42 days) and 30 days (range, 21-54 days) after symptoms onset, respectively. Severe patients in AP and CP were presented as black symbols. (**B**) The expression of CD80 and CD86 on $CD11c^+$ cDC was determined using the MFI by flow cytometry analysis. Enriched DCs of 3 AP (2 severe and 1 mild patients) and 4 mild CP were obtained from samples collected at a median of 11 (range, 1-13 days) and 25 days (range, 21-47 days) after symptoms onset, respectively. DCs were stimulated with the proinflammatory cytokine cocktail (stimuli) for 24 hours before the analysis. Seven HD were included as controls. Secreted levels of IFN-α and IFN-β were determined using the bead-based cytokine assays. (**C**) Enriched DCs derived from the same set of samples in Figure 2B were stimulated with or without the proinflammatory cytokine cocktail (stimuli) for 24 hours, followed by γ-irradiation, and then co-culturing with CFSE-labelled allogeneic T cells from a HD for 5 days. Proliferation of CD4 and CD8 T cells was determined by % CFSE low and analysed by flow cytometry. Each symbol represents an individual donor and the mean of each group are shown. Statistics were generated using one-way ANOVA followed by Tukey's multiple comparisons test Mann–Whitney test and 2-tailed Student's t test. *$p<0.05$; **$p<0.01$, ***$p<0.001$.
See also Figure S2, S3 and Table S1, S2.

**Figure 3. Peripheral T cells display functional loss during acute SARS-CoV-2 infection.** (**A**) Frequencies of $Ki67^+$ cells on CD4 and CD8 T cells were determined by flow cytometry. Fresh PBMCs from 13 AP and 9 CP were collected at a median of 9 (range, 1-20 days) and 31 days (range, 23-54 days) after symptoms onset, respectively. Frequencies of $CD38^+HLA\text{-}DR^+$ and $PD\text{-}1^+$ cells on CD4 T cells (left) and CD8 T cells (right) were also determined by flow cytometry. Samples of 17 AP and 20 CP were collected at a median of 13 (range, 1-42 days) and 29.5 days (range, 21-54 days) after symptoms onset, respectively. Samples of 17 HD were included as controls. Severe patients in AP and CP were presented as black symbols. (**B**) Proliferation ability of T cells from COVID-19 patients was determined by flow cytometry. Fresh PBMCs from 6 AP (1 severe and 5 mild patients) and 6 mild CP

were obtained at a median of 12 (range, 2-25 days) and 32 days (range, 23-39 days) after symptoms onset, respectively. PBMCs were labelled with CFSE and then were cultured in the presence or absences of anti-CD3 and anti-CD28 mAbs for 3 days before the flow cytometry. PBMCs of 6 HD were included as controls. Representative histograms (top-left) and quantified results (top-right panel) depict the CFSE profiles of CD4 and CD8 T cells. The presence of IFN-γ, TNF-α, and IL-2 in culture supernatants after anti-CD3/CD28 stimulation were also quantified using the bead-based cytokine assays (bottom panel). (**C**) T cell responses to non-specific stimulation. Fresh PBMCs (same samples from Figure 4B) were stimulated with PMA/Ionomycin activation cocktail in the presence of BFA for 6 hours. Expressions of IFN-γ and TNF-α in T cells were determined by intracellular cytokine staining analysis. Representative plots showing IFN-γ and TNF-α expression on CD4 and CD8 T cells (Top). Frequencies of IFN-$\gamma^+$ and TNF-$\alpha^+$ cells were gated on CD45RA$^-$ CCR7$^+$ central memory (CM) and CD45RA$^-$CCR7$^-$ effector memory (EM) CD4 T cells (middle), as well as on EM and CD45RA$^+$CCR7$^-$ (CD45RA$^+$ effector memory, EMRA) CD8 T cells (bottom). (**D**) Expression of granzyme B and perforin in unstimulated EM and EMRA CD8 T cells (same samples from Figure 4B) was determined by intracellular staining. Representative plots (top) and quantified results (bottom) are shown. Each symbol represents an individual donor the mean of each group are shown. Statistics were generated using one-way ANOVA followed by Tukey's multiple comparisons test Mann–Whitney test and 2-tailed Student's t test. *p<0.05; **p<0.01, ***<0.001.

See also Figure S1, S4 and Table S1, S2.

**Figure 4. Impact of disease severity on AP-derived immune cells**

Samples of 11 mild and 6 severe acute patients (same as Figure 1 and 2) were collected at a median of 9 (range, 3-23 days) and 15 days (range, 1-54 days) after symptoms onset, respectively. (**A**) The frequencies of lymphocyte subsets (T, B and NK cells) and myeloid cells (DCs, CD14$^{++}$CD16$^-$ monocytes and MDSCs) were analyzed by flow cytometry. (**B**) Frequencies of CD11c$^+$ cDC and CD123$^+$ pDC in total blood DC, and the cDC:pDC ratios were determined by flow cytometry. The expression of HLA-DR, CD86 and CCR2 on cDCs were analysed using the mean fluorescence intensity (MFI). Each symbol represents an individual donor with a line indicating the mean of each group. Statistics were generated using 2-tailed Student's t test. *p<0.05, **p<0.01.

See also Figure S5 and Table S1, S2.

**Figure 5. Timely inverted RBD-specific antibody and T cell responses during acute infection.** (**A**) Neutralising antibody (Nab) responses, shown as $IC_{50}$, of 17 acute patients were measured by a pseudovirus-based assay. Endpoint titers of RBD IgG in plasma of each patient was measured by ELISA. Antigen-specific T cell responses towards the RBD peptide pool and NP protein were determined by the IFN-γ ELISPOT assays. Patient IDs highlighted in bold represent severe patients. (**B**) Percentages of patients with positive RBD IgG, neutralization antibody, NP ELISPOT and RBD ELISPOT responses in each week after symptoms onset according to results in Figure 5A. "NA" means that samples were not available. (**C**) Kinetics of viral loads, anti-RBD IgG, neutralization antibody and T cell responses against RBD peptide pool and NP protein were presented by weeks. Each symbol represents an individual subject. The mean values of individual groups are indicated by bars. Undetectable viral titers and immune responses were set as 1 $Log_{10}$. "NA" means that samples were not available. Severe patients were labelled by black symbols. (**D**) Comparisons of titers of anti-RBD IgG, neutralization antibody, T cell responses against RBD peptide pool and NP protein between mild and severe acute patients with either undetectable (neg) or positive (pos) viral loads. Severe patients were labelled by black symbols. Negative response was set as 1 $Log_{10}$. Each symbol represents an individual subject and the mean values of each group are shown by bars.
See also Figure S6, S7 and Table S1, S3.

**Figure 6. Antibody and T cell response profile of convalescent patients.** (**A**) The NAb $IC_{50}$ of 23 convalescent patients were measured by the pseudovirus-based assay, and the endpoint titer of RBD IgG in plasma of each patient was measured by ELISA. Antigen-specific T cell responses towards the RBD peptide pool and NP protein were determined by IFN-γ ELISPOT respectively. Patient ID highlighted in bold represent severe patients. (**B**) PBMCs from 3 AP and 13 CP were subjected to the ICS assay against RBD peptide pool and NP protein. IFN-$\gamma^+$ cells were gated on CD4 and CD8 T cells, respectively. Representative dot plots (left) and quantified results (right) depict the percentage of IFN-$\gamma^+$ cells. Each symbol represents an individual donor with a line indicating the mean of each group. (**C**) Phenotypes of RBD and NP-specific CD4 T cells were defined using CD45RA and CCR7 markers (left). Averaged frequencies of each subset of IFN-$\gamma^+$ cells were shown (right). Statistics were generated using 2-tailed Student's t test. *$p<0.05$.
See also Figure S7, S8 and Table S1, S3.

**Table 1. Clinical characteristics of all patients in this study.**

## STAR METHODS

### RESOURCE AVAILABILITY

#### Lead Contact

Further information and requests for resources and reagent should be directed to and will be fulfilled by the Lead Contact, Zhiwei Chen (zchenai@hku.hk).

#### Materials Availability

This study did not generate new unique reagents.

#### Data and Code Availability

The study did not generate any unique datasets or codes.

### EXPERIMENTAL MODELS AND SUBJECT DETAILS

#### Human subjects

Forty-one adult COVID-19 patients, including 17 acute and 24 convalescent cases, were recruited from Queen Mary Hospital, Princess Margaret Hospital and Pamela Youde Nethersole Eastern Hospital in the Hong Kong Special Administrative Region. COVID-19 was confirmed by the detection of SARS-CoV-2 by reverse-transcription polymerase chain reaction (RT-PCR) as previously described (To et al., 2020). Twenty-seven out of 39 patients included in this study have been reported recently (Hung et al., 2020), but their immune profiles and functions have not been studied. Written informed consent was obtained from all patients. This study was approved by the Institutional Review Board of University of Hong Kong/Hospital Authority Hong Kong West Cluster, Hong Kong East Cluster Research Ethics Committee, and Kowloon West Cluster Research Ethics Committee (UW 13-265, HKECREC-2018-068, KW/EX-20-038[144-26]). Six severe and 11 mild patients, who remained hospitalized during study, were recruited in the acute patient (AP) group. Blood samples were collected at the median 13.5 days after symptom onset (range, 1-42 days). A

total of 28 blood samples were collected from the AP cohort, of which 21 samples were collected within 21 days after symptom onset and 7 samples were collected at least 21 days after symptom onset. Among the convalescent patients (CP) who received treatment and were subsequently discharged from the hospital, a total of 29 blood samples from 3 severe and 26 mild patients were collected at the median 30 days (range, 21-54 days) after symptoms onset. Patient information of the overall cohort, including age, sex, and health status, was shown in Table 1. A comparison of patient information between acute patients and convalescent patients was shown in Table S1. Healthy human blood buffy coats were obtained from the Red Cross of Hong Kong from donors at median age of 40 (interquartile range, 19-49). The use of buffy coats received ethics approval from the Institutional Review Board of the University of Hong Kong/Hospital Authority Hong Kong West Cluster #UW13-476.

**Cell lines**

HEK 293T-hACE2 cells were maintained in DMEM containing 10% FBS, 2 mM L-glutamine and 100 U/mL penicillin and were incubated at 37□ in 5% $CO_2$ setting (Liu et al., 2019).

## METHOD DETAILS

**Peripheral blood mononuclear cell (PBMC) isolation**

PBMCs from healthy donors and patients were isolated from fresh blood samples using Ficoll-Paque density gradient centrifugation in our BSL-3 laboratory at the same day of blood collection. The majority of purified PBMCs were used for immune cell phenotyping whereas plasma samples were subjected to antibody testing. The rest of the cells were cryopreserved in freezing medium (90% FBS+10% DMSO) at $5\times10^6$ cells/mL at -150□.

**The 12-color flow cytometry analysis**

For the 12-color flow cytometry analysis, four panels of mAbs were used (Biolegend, eBiosciences and BD Biosciences) (Table S2). Cells were incubated for 10 minutes with Fc Block (BD Biosciences) in staining buffer (PBS containing 2% FBS) followed by staining with the indicated antibodies for 30 minutes at 4□. The amounts of cytokines of interest in culture supernatant were measured by LEGENDplex Human Panel (13-plex, Biolegend). Stained cells and beads were acquired by FACSAriaIII Flow Cytometer (BD Biosciences)

inside a BSL-3 laboratory and analyzed with FlowJo software (v10.6) (BD Bioscience) and LEGENDplex software (v8.0) (Biolegend).

**Dendritic cell (DC) isolation and *in vitro* maturation**

Mixed population of pDC and mDC were firstly isolated using untouched Pan-DC Enrichment Kits (Miltenyi Biotec) according to manufacturer's instructions and were then cultured in AIM-V medium (Gibco). For the maturation assay, DCs were stimulated with a cocktail of proinflammatory cytokines (10 ng/mL of recombinant human IL-1β, IL-6, TNF-α and 500 ng/mL of prostaglandin E2 for 24 hours as previously described (Schuler-Thurner et al., 2002). The expression of DC maturation markers was then determined by flow cytometry.

**Allogeneic mixed lymphocyte reaction assay (MLR)**

Pan DCs were stimulated with or without the cocktail of proinflammatory cytokines for 24 hours and were then washed 3 times with PBS. DCs were then γ-irradiated (30 Gy) and counted using trypan blue. Pan T cells from allogeneic healthy donors were isolated using a human Pan T Cell Isolation Kit according to manufacturer's instructions. T cells were then stained with 5 µM Carboxyfluorescein succinimidyl ester (CFSE) for 10 min and further washed 3 times with medium (AIM-V). $1x10^4$ viable DCs from either HD or patients were co-cultured with CFSE-labelled allogeneic T cells ($10^5$) from a different HD at a DC:T cells ratio of 1:10. T cells alone and T cells stimulated with anti-CD3/CD28 mAbs were included as the negative and positive controls, respectively. Five days post-coculture, the percentage of T cell proliferation was measured by CFSE dilution as previously described (Gutzmer et al., 2004).

**T cell proliferation**

To measure T cell proliferation, Carboxyfluorescein 6 succinimidyl ester (CFSE, Thermo Scientific)-labelled PBMCs were cultured in 96-well U-bottom plates with RPMI 1640 medium containing 10% FBS and 1% streptomycin/penicillin (all from Gibco). PBMCs were then cultured in the presence or absence of soluble anti-CD3 (2 µg/mL) antibody and anti-CD28 (1 µg/mL) antibody for 3 days. Proliferated T cells were identified by CFSE dilution.

**Intracellular cytokine staining (ICS)**

To measure T cell activation, PBMCs were stimulated with the commercially available cell activation cocktail (Biolegend) containing phorbol 12-myristate-13-acetate (PMA) and

ionomycin in the presence of brefeldin A (BFA, 7.5 µg/mL, Sigma-Aldrich) for 6 h. For COVID-19-specific T cell responses, PBMCs were stimulated with 1 µg/mL COVID-19 RBD peptide pool (15-mer overlapping by 11, spanning the whole RBD sequence at $Spike_{306-543}$) or 5 µg/mL purified nucleocapsid (NP) protein in the presence of 0.5 µg/mL anti-CD28 and anti-CD49d mAbs (BD Bioscience). Cells were incubated at 37□ overnight and BFA was added at 2 hours post incubation, as previously described (Li et al., 2008a). PMA/ionomycin stimulation was included as positive control. After overnight incubation, cells were washed with staining buffer (PBS containing 2% FBS) and stained with mAbs against surface markers. For intracellular staining, cells were fixed and permeabilized with BD Cytofix/Cytoperm (BD Biosciences) prior to staining with the mAbs against cytokines (Table S2). Results were considered positive when there was at least a 2-fold increase above the background of HD.

**IFN-γ ELISPOT**

Frozen PBMCs were rested overnight at 37□ with 5% $CO_2$ after thawing. Cells were then seeded into the anti-human IFN-γ mAb pre-coated 96-well plate at 200,000 cells/well. The COVID-19 RBD peptide pool using the optimal concentration of 1 µg/mL (Grifoni, 2020) or NP protein (5 µg/mL) was added to the cells for overnight incubation in the presence of anti-CD28 and anti-CD49d mAbs (0.5 µg/mL) as described by others (Li et al., 2008b; Shin et al., 2019; Waldrop et al., 1998). The sequences of the RBD peptide pool are shown in Table S3. PMA/ionomycin treatment was used as the positive control and anti-CD28/anti-CD49d mAbs treatment was used as the as the negative control. The ELISPOT assay was performed using the human IFN-γ ELISPOT Kit (Mabtech) according the manufacturer's instructions. Spots were counted using an immunospot reader and image analyzer (Cellular Technology Limited). Results were considered positive when the number of spot-forming cells (SFC)/$10^6$ PBMCs was 2-fold above that of the negative controls.

**Pseudotyped viral neutralization assay**

To determine the neutralizing activity of patients' plasma, plasma were inactivated at 56□ for 30 min prior to a pseudotype viral entry assay as previously described (Liu et al., 2019; Zhang et al., 2006). The result of this assay is strongly correlated with that of neutralization assay using replication-competent SARS-CoV or SARS-CoV-2 (Liu et al., 2020; Temperton et al., 2005). In brief, the SARS-CoV-2 pseudotype virus was generated through co-transfection of 293T cells with 2 plasmids, pVax-1-S-COVID19 and pNL4-3Luc_Env_Vpr,

carrying the optimized SARS-CoV-2 S gene and a human immunodeficiency virus type 1 backbone respectively. At 48 hours post-transfection, viral supernatant was collected and frozen at -150°C. Serially diluted serum samples were incubated with 200 $TCID_{50}$ of pseudovirus at 37°C for 1 hour. The serum-virus mixtures were then added into pre-seeded HEK 293T-hACE2 cells. After 48 hours, infected cells were lysed and luciferase activity was measured using Luciferase Assay System kits (Promega) in a Victor3-1420 Multilabel Counter (PerkinElmer). The 50% inhibitory concentrations ($IC_{50}$) of each serum specimen were calculated to reflect anti-SARS-CoV-2 potency.

**Enzyme-linked immunosorbent assay (ELISA)**

ELISA was performed to detect SARS-CoV-2 RBD-specific IgG, as previously described (Wu et al., 2018). In brief, 96-well plates (Costar) were coated with recombinant SARS-CoV-2 RBD antigen (50 ng/well; Sino Biological) at 4°C overnight. After washing with PBST (0.05% Tween-20 in PBS), the plates were blocked with 4% skim milk in PBS for 1 hour at 37°C and incubated with serially diluted patient plasma for 1 hour at 37°C. After washing with PBST, goat anti-human IgG conjugated with HRP (Santa Cruz Biotechnology) was added and the whole solution was incubated for 1 hour, followed by washing and the addition of 50 µl HRP chromogenic substrate 3,3',5,5'-TMB (Sigma). Optical density (OD) values were measured at 450 nm using the VARIOSKANTM LUX multimode microplate reader (Thermo Fisher Scientific). Five-fold of mean OD values detected from blank wells containing 4% skim milk in PBS alone was used as a cutoff for the endpoint antibody titer calculation. All experiments were performed in duplicate.

**Real-time RT-PCR assay for SARS-CoV-2 RNA measurement**

Saliva specimens from COVID-19 patients were collected as previously described (To et al., 2020) and further subjected to total nucleic acid (TNA) extraction using a NucliSENS easyMAG extraction system (Chan et al., 2020b). The real-time RT-PCR assay for SARS-CoV-2-RdRp/Hel RNA detection was performed using QuantiNova Probe RT-PCR kit (Qiagen) in a LightCycler 480 real-time PCR system. Briefly, 5 µl TNA was added to 15 µl reaction mixture that contained 10 µM probe. The thermal cycling condition was 10 min at 45°C for reverse transcription, 5 min at 95°C for PCR initial activation, and 45 cycles of 5 s at 95°C and 30 s at 55°C.

**QUANTIFICATION AND STATISTICAL ANALYSIS**

Statistical analysis was performed with the GraphPad Prism 6 Software. Data represent mean values or mean values with SD. Significant differences between the means of three groups were tested using a one-way analysis of variance (ANOVA) followed by Tukey's multiple comparisons test. Significant differences between two groups were performed using the 2-tailed Student's t test. $P < 0.05$ was considered statistically significant.

**Table S1. Comparison between patients with acute samples (collected during hospitalization) and those with convalescent samples (collected at out-patient clinic). Related to Figure 1-6.**

**Table S2. Four Panels of antibodies for flow cytometry analysis. Related to Figure 1-4.**

**Table S3. List of the SARS-CoV-2 RBD peptide pool (15-mer overlapping by 11, spanning the whole RBD sequence at Spike306-543) used in this study. Related to Figure 5 and 6.**

## References


Blanco-Melo, D., Nilsson-Payant, B.E., Liu, W.C., Uhl, S., Hoagland, D., Moller, R., Jordan, T.X., Oishi, K., Panis, M., Sachs, D., *et al.* (2020). Imbalanced Host Response to SARS-CoV-2 Drives Development of COVID-19. Cell.

Chan, J.F., Kok, K.H., Zhu, Z., Chu, H., To, K.K., Yuan, S., and Yuen, K.Y. (2020a). Genomic characterization of the 2019 novel human-pathogenic coronavirus isolated from a patient with atypical pneumonia after visiting Wuhan. Emerg Microbes Infect *9*, 221-236.

Chan, J.F., Yip, C.C., To, K.K., Tang, T.H., Wong, S.C., Leung, K.H., Fung, A.Y., Ng, A.C., Zou, Z., Tsoi, H.W., *et al.* (2020b). Improved Molecular Diagnosis of COVID-19 by the Novel, Highly Sensitive and Specific COVID-19-RdRp/Hel Real-Time Reverse Transcription-PCR Assay Validated In Vitro and with Clinical Specimens. J Clin Microbiol *58*.

Channappanavar, R., Fett, C., Zhao, J., Meyerholz, D.K., and Perlman, S. (2014). Virus-specific memory CD8 T cells provide substantial protection from lethal severe acute respiratory syndrome coronavirus infection. J Virol *88*, 11034-11044.

Chaplin, D.D. (2010). Overview of the immune response. J Allergy Clin Immunol *125*, S3-23.

Chen, H., Hou, J., Jiang, X., Ma, S., Meng, M., Wang, B., Zhang, M., Zhang, M., Tang, X., Zhang, F., *et al.* (2005). Response of memory CD8+ T cells to severe acute respiratory syndrome (SARS) coronavirus in recovered SARS patients and healthy individuals. J Immunol *175*, 591-598.

Chen, J., Qi, T., Liu, L., Ling, Y., Qian, Z., Li, T., Li, F., Xu, Q., Zhang, Y., Xu, S., *et al.* (2020a). Clinical progression of patients with COVID-19 in Shanghai, China. J Infect *80*, e1-e6.

Chen, N., Zhou, M., Dong, X., Qu, J., Gong, F., Han, Y., Qiu, Y., Wang, J., Liu, Y., Wei, Y., *et al.* (2020b). Epidemiological and clinical characteristics of 99 cases of 2019 novel coronavirus pneumonia in Wuhan, China: a descriptive study. Lancet.

Chiappelli, F., Khakshooy, A., and Greenberg, G. (2020). CoViD-19 Immunopathology and Immunotherapy. Bioinformation *16*, 219-222.

Chu, H., Chan, J.F., Wang, Y., Yuen, T.T., Chai, Y., Hou, Y., Shuai, H., Yang, D., Hu, B., Huang, X., *et al.* (2020). Comparative replication and immune activation profiles of SARS-CoV-2 and SARS-CoV in human lungs: an ex vivo study with implications for the pathogenesis of COVID-19. Clin Infect Dis.

Du, R.H., Liang, L.R., Yang, C.Q., Wang, W., Cao, T.Z., Li, M., Guo, G.Y., Du, J., Zheng, C.L., Zhu, Q., *et al.* (2020). Predictors of Mortality for Patients with COVID-19 Pneumonia Caused by SARS-CoV-2: A Prospective Cohort Study. Eur Respir J.

Fitzgerald-Bocarsly, P., Dai, J., and Singh, S. (2008). Plasmacytoid dendritic cells and type I IFN: 50 years of convergent history. Cytokine Growth Factor Rev *19*, 3-19.

Grifoni, A., Weiskopf, D., Ramirez, S.I., Mateus, J., Dan, J.M., Moderbacher, C.R., Rawlings, S.A., Sutherland, A., Premkumar, L., Jadi, R.S., Marrama, D., de Silva, A.M., Frazier, A., Carlin, A., Greenbaum, J.A., Peters, B., Krammer, F., Smith, D.M., Crotty, S., Sette, A. (2020). Targets of T cell responses to SARS-CoV-2 coronavirus in humans with COVID-19 disease and unexposed individuals. Cell.

Gutzmer, R., Li, W., Sutterwala, S., Lemos, M.P., Elizalde, J.I., Urtishak, S.L., Behrens, E.M., Rivers, P.M., Schlienger, K., Laufer, T.M., *et al.* (2004). A tumor-associated glycoprotein that blocks MHC class II-dependent antigen presentation by dendritic cells. J Immunol *173*, 1023-1032.

Ho, M.S., Chen, W.J., Chen, H.Y., Lin, S.F., Wang, M.C., Di, J., Lu, Y.T., Liu, C.L., Chang, S.C., Chao, C.L., *et al.* (2005). Neutralizing antibody response and SARS severity. Emerg Infect Dis *11*, 1730-1737.
Holshue, M.L., DeBolt, C., Lindquist, S., Lofy, K.H., Wiesman, J., Bruce, H., Spitters, C., Ericson, K., Wilkerson, S., Tural, A., *et al.* (2020). First Case of 2019 Novel Coronavirus in the United States. N Engl J Med.
Huang, C., Wang, Y., Li, X., Ren, L., Zhao, J., Hu, Y., Zhang, L., Fan, G., Xu, J., Gu, X., *et al.* (2020). Clinical features of patients infected with 2019 novel coronavirus in Wuhan, China. Lancet.
Hung, I.F., Lung, K.C., Tso, E.Y., Liu, R., Chung, T.W., Chu, M.Y., Ng, Y.Y., Lo, J., Chan, J., Tam, A.R., *et al.* (2020). Triple combination of interferon beta-1b, lopinavir-ritonavir, and ribavirin in the treatment of patients admitted to hospital with COVID-19: an open-label, randomised, phase 2 trial. Lancet.
Jiang, H.-w., Li, Y., Zhang, H.-n., Wang, W., Men, D., Yang, X., Qi, H., Zhou, J., and Tao, S.-c. (2020). Global profiling of SARS-CoV-2 specific IgG/ IgM responses of convalescents using a proteome microarray. 2020.2003.2020.20039495.
Jongbloed, S.L., Kassianos, A.J., McDonald, K.J., Clark, G.J., Ju, X.S., Angel, C.E., Chen, C.J.J., Dunbar, P.R., Wadley, R.B., Jeet, V., *et al.* (2010). Human CD141(+) (BDCA-3)(+) dendritic cells (DCs) represent a unique myeloid DC subset that cross-presents necrotic cell antigens. J Exp Med *207*, 1247-1260.
Law, H.K., Cheung, C.Y., Ng, H.Y., Sia, S.F., Chan, Y.O., Luk, W., Nicholls, J.M., Peiris, J.S., and Lau, Y.L. (2005). Chemokine up-regulation in SARS-coronavirus-infected, monocyte-derived human dendritic cells. Blood *106*, 2366-2374.
Li, C.K., Wu, H., Yan, H., Ma, S., Wang, L., Zhang, M., Tang, X., Temperton, N.J., Weiss, R.A., Brenchley, J.M., *et al.* (2008a). T cell responses to whole SARS coronavirus in humans. J Immunol *181*, 5490-5500.
Li, C.K.F., Wu, H., Yan, H.P., Ma, S.W., Wang, L.L., Zhang, M.X., Tang, X.P., Temperton, N.J., Weiss, R.A., Brenchley, J.M., *et al.* (2008b). T cell responses to whole SARS coronavirus in humans. Journal of Immunology *181*, 5490-5500.
Liao, M., Liu, Y., Yuan, J., Wen, Y., Xu, G., Zhao, J., Cheng, L., Li, J., Wang, X., Wang, F., *et al.* (2020). Single-cell landscape of bronchoalveolar immune cells in patients with COVID-19. Nat Med *26*, 842-844.
Liu, L., To, K.K., Chan, K.H., Wong, Y.C., Zhou, R., Kwan, K.Y., Fong, C.H., Chen, L.L., Choi, C.Y., Lu, L., *et al.* (2020). High neutralizing antibody titer in intensive care unit patients with COVID-19. Emerg Microbes Infect *9*, 1664-1670.
Liu, L., Wei, Q., Lin, Q., Fang, J., Wang, H., Kwok, H., Tang, H., Nishiura, K., Peng, J., Tan, Z., *et al.* (2019). Anti-spike IgG causes severe acute lung injury by skewing macrophage responses during acute SARS-CoV infection. JCI Insight *4*, e123158.
Liu, L., Wei, Q., Nishiura, K., Peng, J., Wang, H., Midkiff, C., Alvarez, X., Qin, C., Lackner, A., and Chen, Z. (2016). Spatiotemporal interplay of severe acute respiratory syndrome coronavirus and respiratory mucosal cells drives viral dissemination in rhesus macaques. Mucosal Immunol *9*, 1089-1101.
Lv, Y., Ruan, Z., Wang, L., Ni, B., and Wu, Y. (2009). Identification of a novel conserved HLA-A*0201-restricted epitope from the spike protein of SARS-CoV. BMC Immunol *10*, 61.
Mitchison, N.A. (2004). T-cell-B-cell cooperation. Nat Rev Immunol *4*, 308-312.
Ni, L., Ye, F., Cheng, M.L., Feng, Y., Deng, Y.Q., Zhao, H., Wei, P., Ge, J., Gou, M., Li, X., *et al.* (2020). Detection of SARS-CoV-2-Specific Humoral and Cellular Immunity in COVID-19 Convalescent Individuals. Immunity.
Qian, Z.P., Mei, X., Zhang, Y.Y., Zou, Y., Zhang, Z.G., Zhu, H., Guo, H.Y., Liu, Y., Ling, Y., Zhang, X.Y., *et al.* (2020). [Analysis of baseline liver biochemical parameters in 324

cases with novel coronavirus pneumonia in Shanghai area]. Zhonghua Gan Zang Bing Za Zhi *28*, E005.

Rothe, C., Schunk, M., Sothmann, P., Bretzel, G., Froeschl, G., Wallrauch, C., Zimmer, T., Thiel, V., Janke, C., Guggemos, W., *et al.* (2020). Transmission of 2019-nCoV Infection from an Asymptomatic Contact in Germany. N Engl J Med.

Schuler-Thurner, B., Schultz, E.S., Berger, T.G., Weinlich, G., Ebner, S., Woerl, P., Bender, A., Feuerstein, B., Fritsch, P.O., Romani, N., and Schuler, G. (2002). Rapid induction of tumor-specific type 1 T helper cells in metastatic melanoma patients by vaccination with mature, cryopreserved, peptide-loaded monocyte-derived dendritic cells. J Exp Med *195*, 1279-1288.

Shin, H.S., Kim, Y., Kim, G., Lee, J.Y., Jeong, I., Joh, J.S., Kim, H., Chang, E., Sim, S.Y., Park, J.S., and Lim, D.G. (2019). Immune Responses to Middle East Respiratory Syndrome Coronavirus During the Acute and Convalescent Phases of Human Infection. Clinical Infectious Diseases *68*, 984-992.

Tan, W., Lu, Y., Zhang, J., Wang, J., Dan, Y., Tan, Z., He, X., Qian, C., Sun, Q., Hu, Q., *et al.* (2020). Viral Kinetics and Antibody Responses in Patients with COVID-19. 2020.2003.2024.20042382.

Temperton, N.J., Chan, P.K., Simmons, G., Zambon, M.C., Tedder, R.S., Takeuchi, Y., and Weiss, R.A. (2005). Longitudinally profiling neutralizing antibody response to SARS coronavirus with pseudotypes. Emerg Infect Dis *11*, 411-416.

To, K.K., Tsang, O.T., Leung, W.S., Tam, A.R., Wu, T.C., Lung, D.C., Yip, C.C., Cai, J.P., Chan, J.M., Chik, T.S., *et al.* (2020). Temporal profiles of viral load in posterior oropharyngeal saliva samples and serum antibody responses during infection by SARS-CoV-2: an observational cohort study. Lancet Infect Dis *20*, 565-574.

Tseng, C.T., Perrone, L.A., Zhu, H., Makino, S., and Peters, C.J. (2005). Severe acute respiratory syndrome and the innate immune responses: modulation of effector cell function without productive infection. J Immunol *174*, 7977-7985.

Waldrop, S.L., Davis, K.A., Maine, V.C., and Picker, L.J. (1998). Normal human CD4(+) memory T cells display broad heterogeneity in their activation threshold for cytokine synthesis. Journal of Immunology *161*, 5284-5295.

Wan, Y., Shang, J., Graham, R., Baric, R.S., and Li, F. (2020). Receptor recognition by novel coronavirus from Wuhan: An analysis based on decade-long structural studies of SARS. J Virol.

Wang, D., Hu, B., Hu, C., Zhu, F., Liu, X., Zhang, J., Wang, B., Xiang, H., Cheng, Z., Xiong, Y., *et al.* (2020a). Clinical Characteristics of 138 Hospitalized Patients With 2019 Novel Coronavirus-Infected Pneumonia in Wuhan, China. JAMA.

Wang, P., Liu, L., Nair, M.S., Yin, M.T., Luo, Y., Wang, Q., Yuan, T., Mori, K., Solis, A.G., Yamashita, M., *et al.* (2020b). SARS-CoV-2 Neutralizing Antibody Responses Are More Robust in Patients with Severe Disease. bioRxiv, 2020.2006.2013.150250.

Wang, Y.D., Sin, W.Y., Xu, G.B., Yang, H.H., Wong, T.Y., Pang, X.W., He, X.Y., Zhang, H.G., Ng, J.N., Cheng, C.S., *et al.* (2004). T-cell epitopes in severe acute respiratory syndrome (SARS) coronavirus spike protein elicit a specific T-cell immune response in patients who recover from SARS. J Virol *78*, 5612-5618.

Wu, A., Peng, Y., Huang, B., Ding, X., Wang, X., Niu, P., Meng, J., Zhu, Z., Zhang, Z., Wang, J., *et al.* (2020). Genome Composition and Divergence of the Novel Coronavirus (2019-nCoV) Originating in China. Cell Host Microbe.

Wu, X., Guo, J., Niu, M., An, M., Liu, L., Wang, H., Jin, X., Zhang, Q., Lam, K.S., Wu, T., *et al.* (2018). Tandem bispecific neutralizing antibody eliminates HIV-1 infection in humanized mice. J Clin Invest *128*, 2239-2251.

Xu, B., Fan, C.Y., Wang, A.L., Zou, Y.L., Yu, Y.H., He, C., Xia, W.G., Zhang, J.X., and Miao, Q. (2020). Suppressed T cell-mediated immunity in patients with COVID-19: a clinical retrospective study in Wuhan, China. J Infect.

Xu, X., and Gao, X. (2004). Immunological responses against SARS-coronavirus infection in humans. Cell Mol Immunol *1*, 119-122.

Yi, C.E., Ba, L., Zhang, L., Ho, D.D., and Chen, Z. (2005). Single amino acid substitutions in the severe acute respiratory syndrome coronavirus spike glycoprotein determine viral entry and immunogenicity of a major neutralizing domain. J Virol *79*, 11638-11646.

Zhang, L., Zhang, F., Yu, W., He, T., Yu, J., Yi, C.E., Ba, L., Li, W., Farzan, M., Chen, Z., *et al.* (2006). Antibody responses against SARS coronavirus are correlated with disease outcome of infected individuals. J Med Virol *78*, 1-8.

Zhang, Z., Wang, F.S., Zhao, M., Liu, J.C., Xu, D.P., Jin, L., Chen, J.M., Wang, M., and Chu, F.L. (2004). [Characterization of peripheral dendritic cell subsets and its implication in patients infected with severe acute respiratory syndrome]. Zhonghua Yi Xue Za Zhi *84*, 22-26.

Zhao, J., Zhao, J., and Perlman, S. (2010). T cell responses are required for protection from clinical disease and for virus clearance in severe acute respiratory syndrome coronavirus-infected mice. J Virol *84*, 9318-9325.

Zheng, Y., Xu, H., Yang, M., Zeng, Y., Chen, H., Liu, R., Li, Q., Zhang, N., and Wang, D. (2020). Epidemiological characteristics and clinical features of 32 critical and 67 noncritical cases of COVID-19 in Chengdu. J Clin Virol *127*, 104366.

Zhu, N., Zhang, D., Wang, W., Li, X., Yang, B., Song, J., Zhao, X., Huang, B., Shi, W., Lu, R., *et al.* (2020). A Novel Coronavirus from Patients with Pneumonia in China, 2019. N Engl J Med.

**Highlights:**

1. Acute SARS-CoV-2 infection results in broad immune cell reduction
2. Both dendritic cells and T cells are functionally impaired
3. Neutralizing antibodies are rapidly and abundantly generated
4. RBD- and NP-specific T cells are delayed at the acute stage

**eTOC (Less than 50 words)**

COVID-19 is an acute disease caused by SARS-CoV-2 infection. We determine how immune system responds to SARS-CoV-2 at both acute and convalescent stages. Acute SARS-CoV-2 infection results in broad immune cell reduction and functional impairment. While neutralizing antibodies are rapidly generated, antigen-specific T cells are delayed at the acute stage.

**Table 1. Clinical characteristics of all patients in this study**

| Characteristics | Severe (n=8) | Mild (n=33) | P value |
|---|---|---|---|
| **Demographic** | | | |
| Age, median years (interquartile range) | 59 (54.5-69.5) | 52 (33.5-63) | 0.137 |
| Female | 4 (50) | 20 (60.6) | 0.698 |
| | | | |
| **Chronic comorbidities** | | | |
| Hypertension | 4 (50) | 4 (12.1) | 0.033 |
| Chronic heart disease | 0 (0) | 1 (3.0) | 1.000 |
| Chronic lung disease | 0 (0) | 1 (3.0) | 1.000 |
| Chronic liver disease | 1 (12.5) | 1(21.5) | 0.195 |
| Chronic kidney disease | 0 (0) | 0 (0) | NA |
| Diabetes mellitus | 3 (37.5) | 2 (6.1) | 0.043 |
| Any chronic comorbidities | 6 (75) | 9 (27.3) | 0.035 |
| | | | |
| **Presenting symptoms** | | | |
| Fever | 6 (75) | 17 (51.5) | 0.429 |
| Dyspnea | 3 (37.5) | 2 (6.1) | 0.043 |
| Cough | 5 (62.5) | 11 (33.3) | 0.225 |
| Rhinorrhea | 1 (12.5) | 3 (9.1) | 1.000 |
| Sore throat | 2 (25) | 4 (12.1) | 0.578 |
| Diarrhoea | 2 (25) | 2 (6.1) | 0.165 |
| | | | |
| **Blood tests on admission**, (median, interquartile range) | | | |
| Haemoglobin (g/dL) | 13.0 (12.5-14.6) | 13.5 (12.7-14.3) | 0.711 |
| Total white blood cell count ($\times 10^9$/L) | 5.0 (4.5-8.2) | 5.3 (4.4-7.4) | 0.885 |
| Neutrophil count ($\times 10^9$/L) | 3.8 (3.2-5.7) | 3.4 (2.2-5.2)[a] | 0.475 |
| Lymphocyte count ($\times 10^9$/L) | 0.9 (0.8-0.9) | 1.2 (1.0-1.6)[a] | 0.011 |
| Platelet count ($\times 10^9$/L) | 150 (141-191) | 236 (184-309)[a] | 0.002 |
| Urea (mmol/L)[b] | 4.4 (3.6-6.2) | 4.0 (3.3-4.9) | 0.325 |
| Creatinine (μmol/L)[b] | 77 (62-94) | 68 (56-86) | 0.496 |
| Alanine aminotransferase (U/L) | 31 (27-59) | 23 (15-33) | 0.065 |
| | | | |
| **Severity** | | | |
| Oxygen supplementation | 8 (100) | 0 (0) | <0.001 |

[a] Neutrophil count, lymphocyte count, urea, creatinine, and alanine aminotransferase available for 32 patients

NA, not applicable

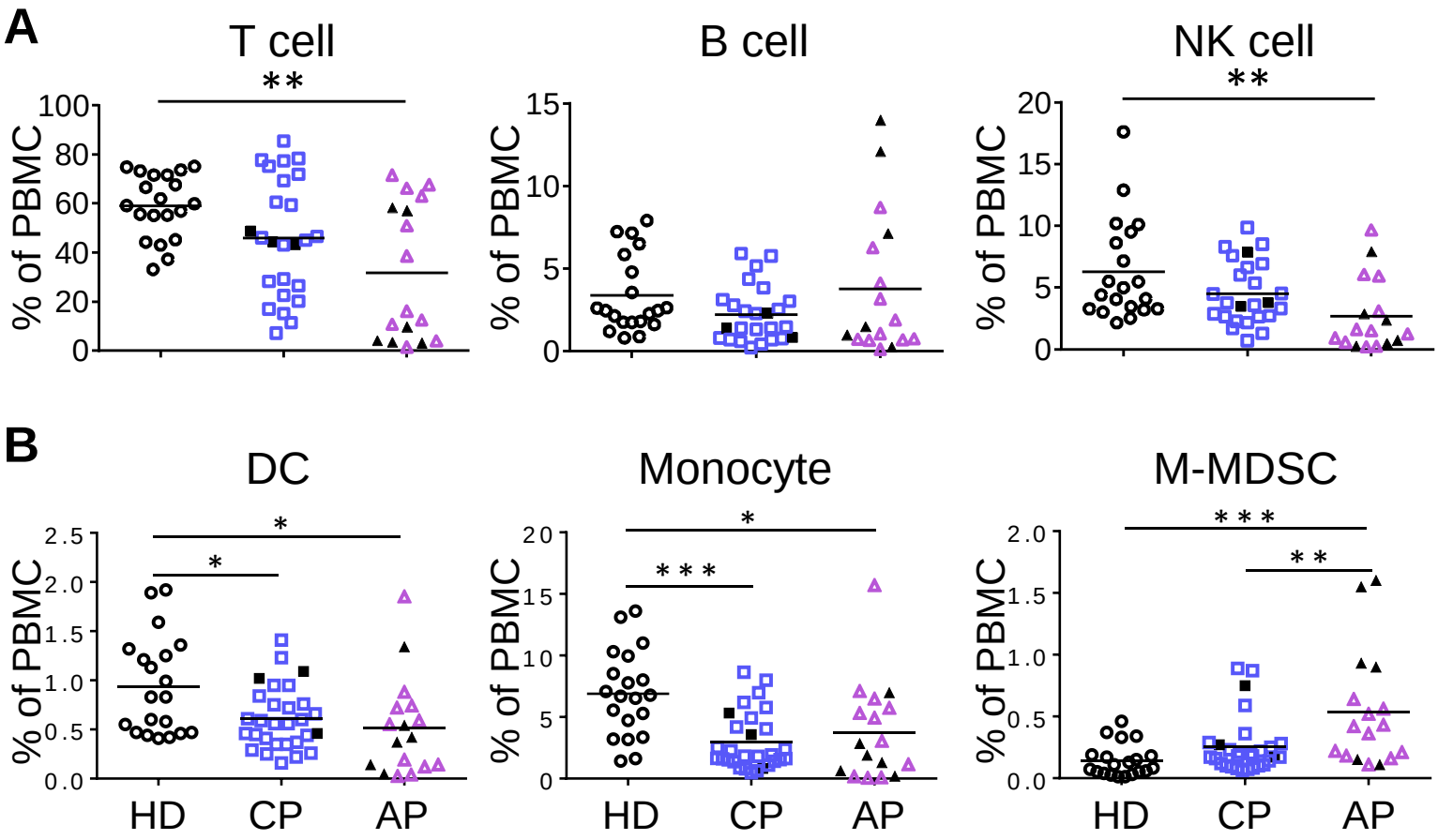
A
T cell
B cell
NK cell
% of PBMC
**
B
DC
Monocyte
M-MDSC
*
***
HD
CP
AP

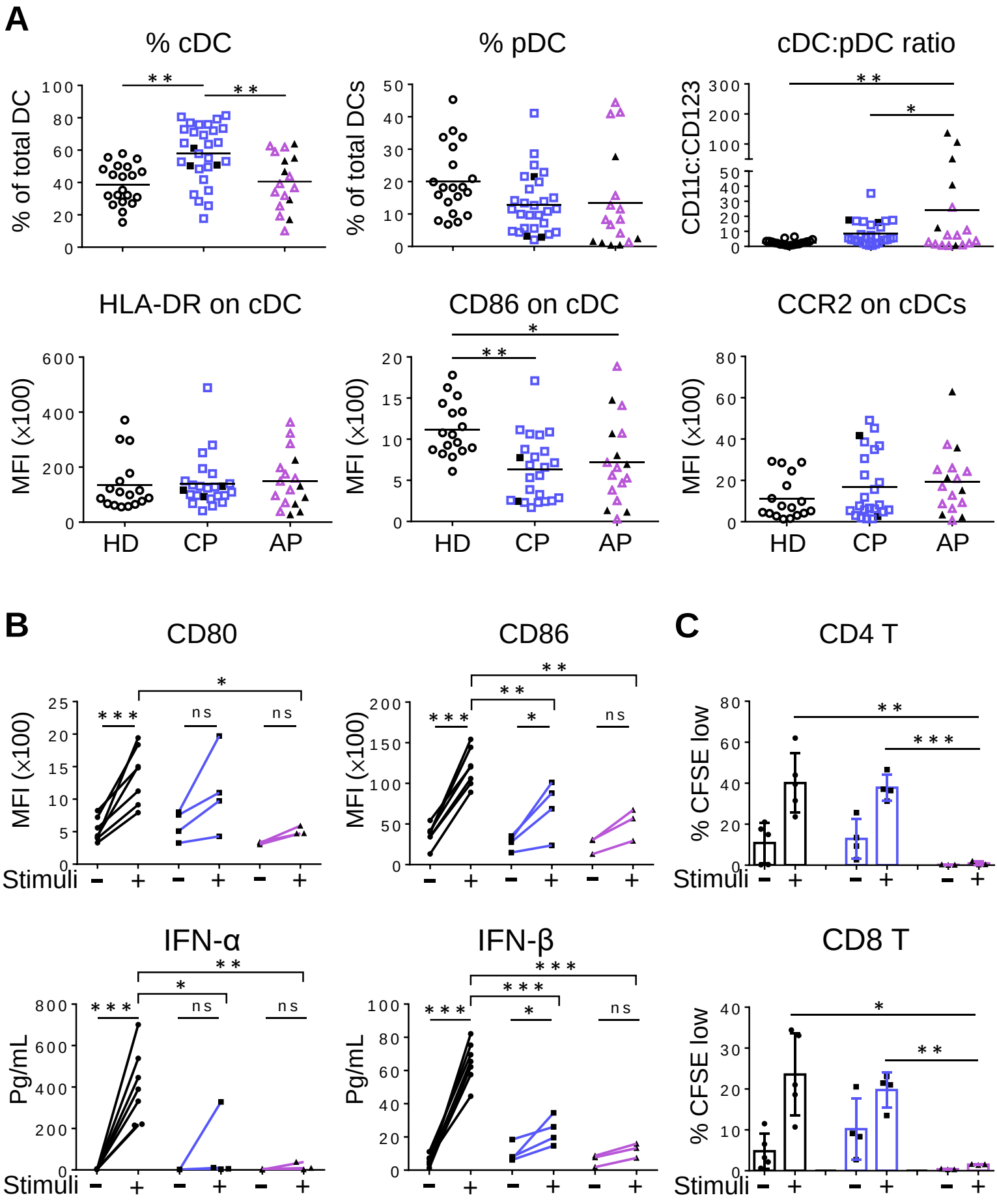
A
% cDC
% of total DC
% pDC
% of total DCs
cDC:pDC ratio
CD11c:CD123
HLA-DR on cDC
MFI (×100)
CD86 on cDC
CCR2 on cDCs
HD
CP
AP
B
CD80
CD86
Stimuli
IFN-α
IFN-β
Pg/mL
C
CD4 T
CD8 T
% CFSE low

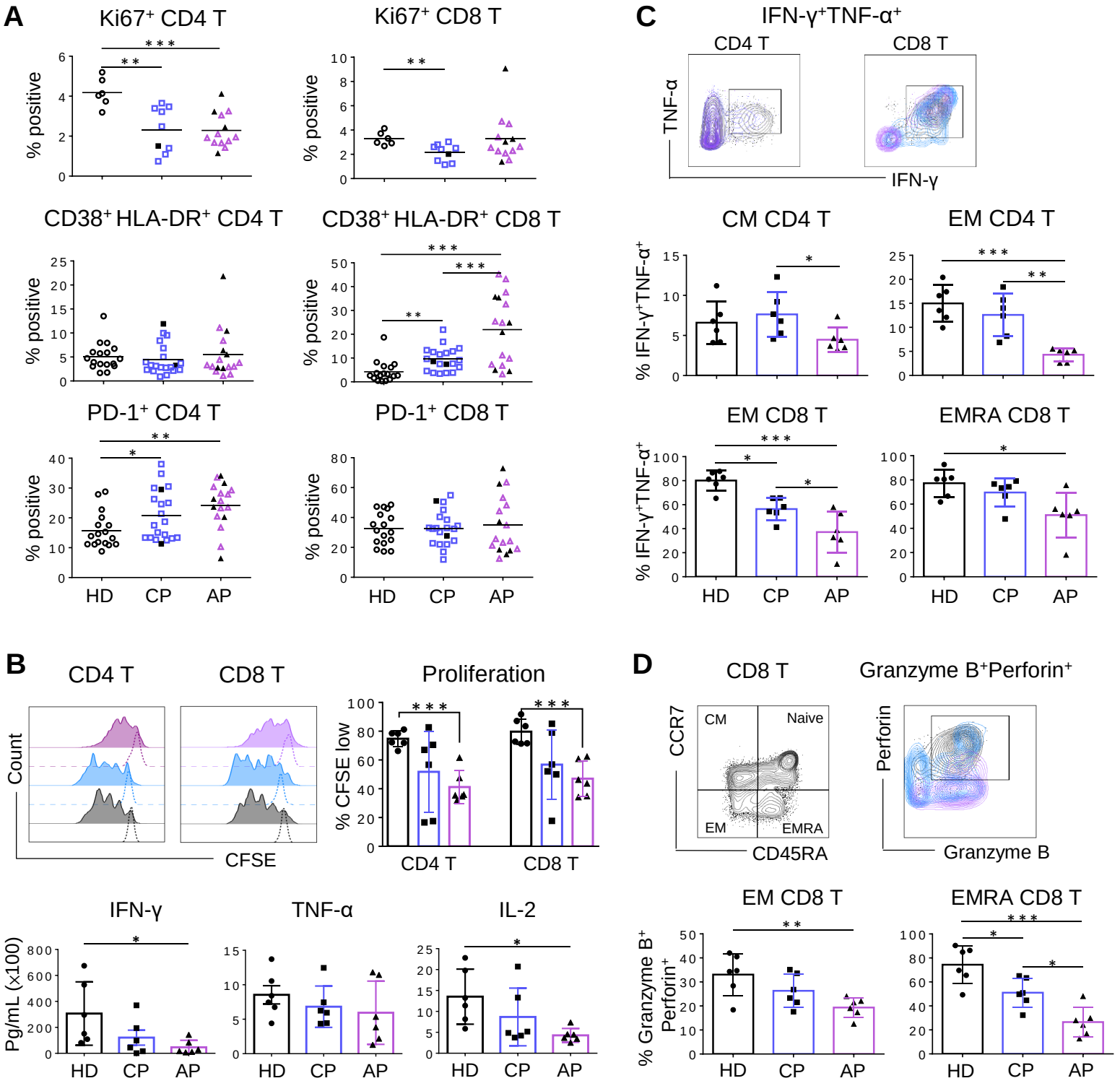
A
Ki67+ CD4 T
Ki67+ CD8 T
% positive
CD38+ HLA-DR+ CD4 T
CD38+ HLA-DR+ CD8 T
PD-1+ CD4 T
PD-1+ CD8 T
HD
CP
AP
C
IFN-γ+TNF-α+
CD4 T
CD8 T
TNF-α
IFN-γ
CM CD4 T
EM CD4 T
% IFN-γ+TNF-α+
EM CD8 T
EMRA CD8 T
B
CD4 T
CD8 T
Count
CFSE
Proliferation
% CFSE low
IFN-γ
TNF-α
IL-2
Pg/mL (x100)
D
CD8 T
Granzyme B+Perforin+
CCR7
CM
Naive
EM
EMRA
CD45RA
Perforin
Granzyme B
% Granzyme B+ Perforin+

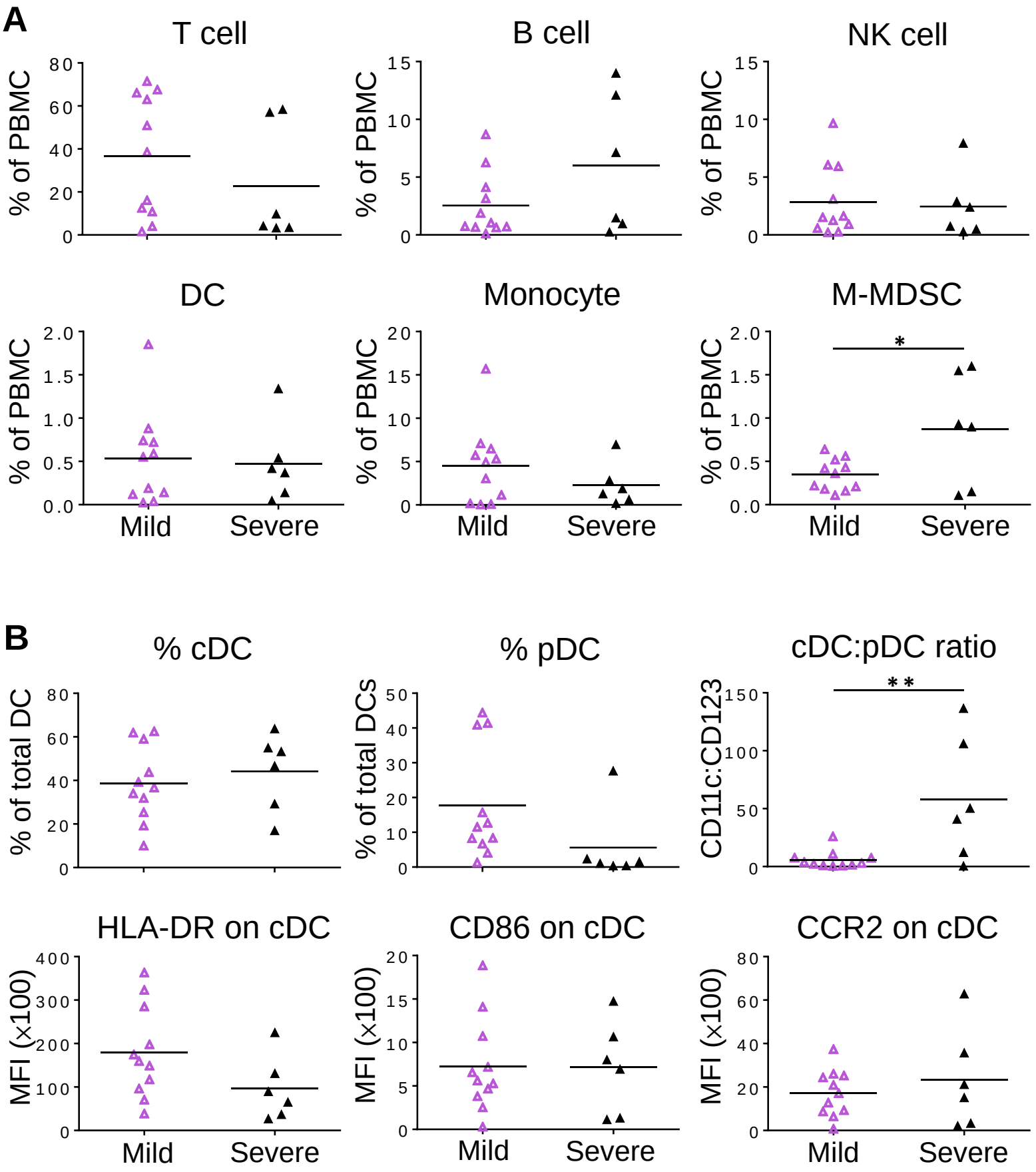
A
T cell
B cell
NK cell
DC
Monocyte
M-MDSC
% of PBMC
Mild
Severe
*
B
% cDC
% pDC
cDC:pDC ratio
% of total DC
% of total DCs
CD11c:CD123
**
HLA-DR on cDC
CD86 on cDC
CCR2 on cDC
MFI (x100)

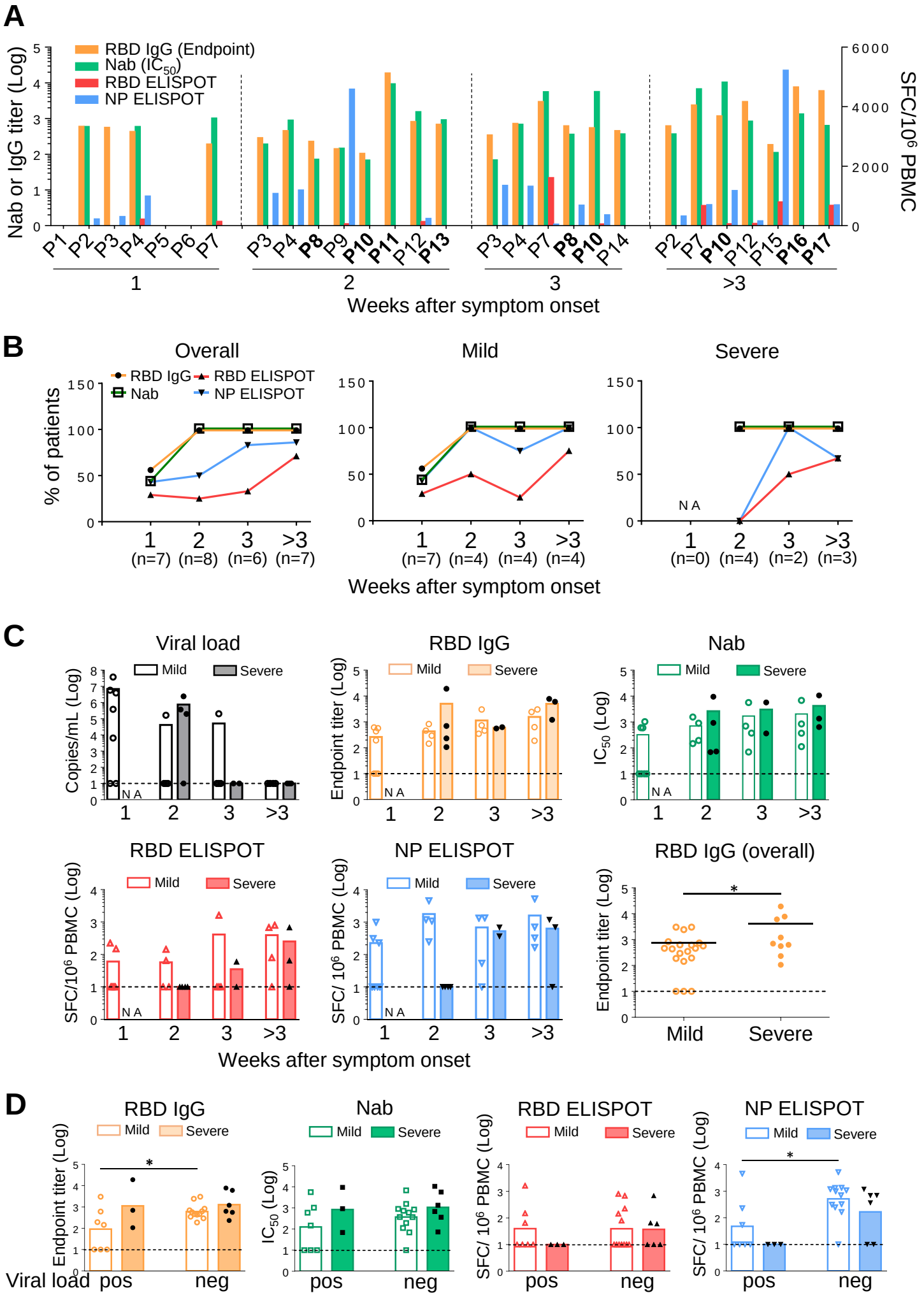
A
RBD IgG (Endpoint)
Nab (IC50)
RBD ELISPOT
NP ELISPOT
Nab or IgG titer (Log)
SFC/10^6 PBMC
P1 P2 P3 P4 P5 P6 P7
P3 P4 P8 P9 P10 P11 P12 P13
P3 P4 P7 P8 P10 P14
P2 P7 P10 P12 P15 P16 P17
1
2
3
>3
Weeks after symptom onset
B
Overall
Mild
Severe
RBD IgG
RBD ELISPOT
Nab
NP ELISPOT
% of patients
N A
1 2 3 >3
(n=7) (n=8) (n=6) (n=7)
(n=7) (n=4) (n=4) (n=4)
(n=0) (n=4) (n=2) (n=3)
Weeks after symptom onset
C
Viral load
RBD IgG
Nab
Copies/mL (Log)
Endpoint titer (Log)
IC50 (Log)
RBD ELISPOT
NP ELISPOT
RBD IgG (overall)
SFC/10^6 PBMC (Log)
SFC/ 10^6 PBMC (Log)
Mild
Severe
N A
*
Weeks after symptom onset
D
RBD IgG
Nab
RBD ELISPOT
NP ELISPOT
Endpoint titer (Log)
IC50 (Log)
SFC/ 10^6 PBMC (Log)
Viral load pos neg
pos neg
*

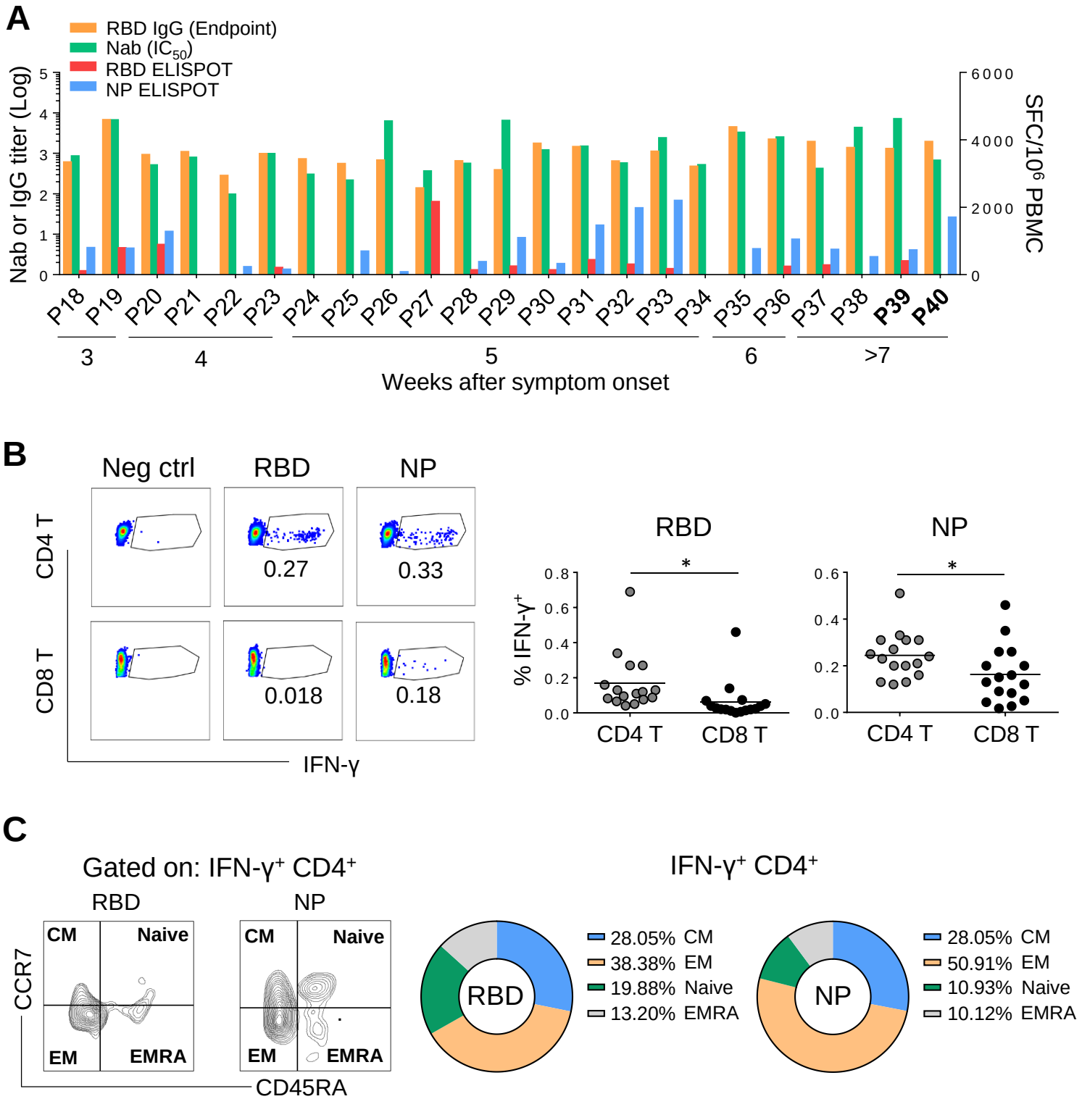
A
RBD IgG (Endpoint)
Nab (IC50)
RBD ELISPOT
NP ELISPOT
Nab or IgG titer (Log)
SFC/10⁶ PBMC
P18 P19 P20 P21 P22 P23 P24 P25 P26 P27 P28 P29 P30 P31 P32 P33 P34 P35 P36 P37 P38 P39 P40
3 4 5 6 >7
Weeks after symptom onset
B
Neg ctrl
RBD
NP
CD4 T
CD8 T
0.27
0.33
0.018
0.18
IFN-γ
RBD
NP
% IFN-γ+
CD4 T
CD8 T
C
Gated on: IFN-γ+ CD4+
RBD
NP
CCR7
CD45RA
CM
Naive
EM
EMRA
IFN-γ+ CD4+
28.05% CM
38.38% EM
19.88% Naive
13.20% EMRA
28.05% CM
50.91% EM
10.93% Naive
10.12% EMRA